Table 2 Reactions of PD 404182 derivatives under reductive conditions in the presence of GSH

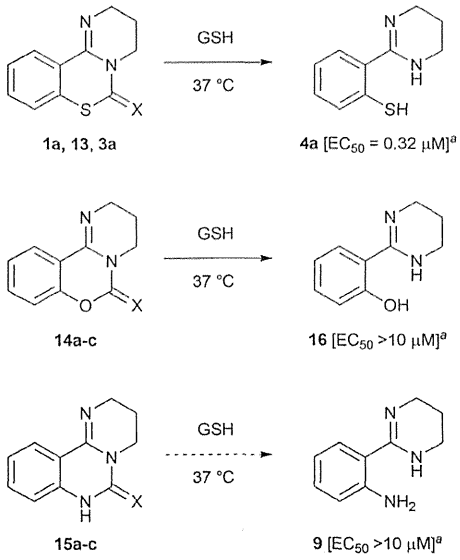

Cmpd	X	EC_{50} [b,7] (μM)	Conversion (time, yield[c])
PD 404182 (**1a**)	NH	0.44 ± 0.08	**4a** (1 h, quant.)
13	O	8.94 ± 1.07	**4a** (24 h, 26%)[d]
3a	S	>10	**4a** (24 h, 15%)[d]
14a	NH	>10	**16** + **14b**[e]
14b	O	>10	**16** (24 h, 78%)
14c	S	>10	**16** (24 h, 71%)
15a	NH	>10	No reaction
15b	O	>10	No reaction
15c	S	>10	No reaction

[a] EC_{50} values represent the concentration of the compound required to inhibit the HIV-1 infection by 50%. The data were obtained from three independent experiments by the NCK assay. [b] EC_{50} values were obtained by the MAGI assay. [c] The product yields were calculated by HPLC analysis using previously determined calibration curves. [d] The reactions were also carried out in the absence of GSH: 5% conversion from **13** after 24 h; no reaction from **3a**. [e] The accurate product yields of **14b** and **16** by GSH-mediated conversion were not calculated because of the chemical instability of the substrate **14a**.

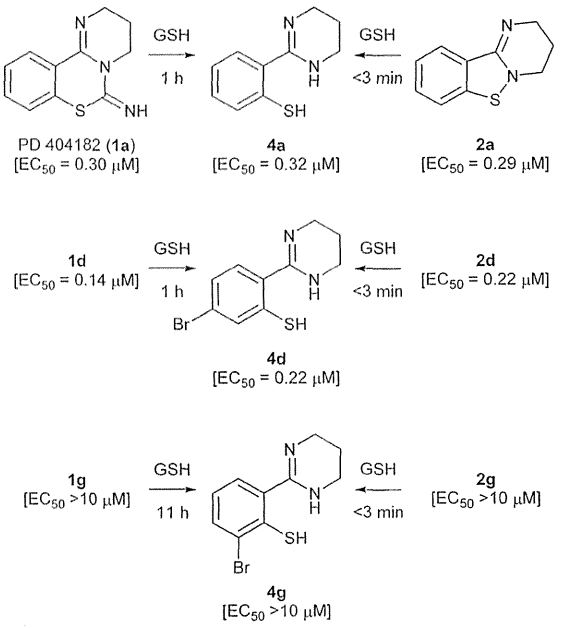

Fig. 4 Reactions of potent and inactive pyrimido[1,2-c][1,3]benzothiazin-6-imine and benzo[4,5]isothiazolo[2,3-*a*]pyrimidine derivatives under reductive conditions in the presence of GSH at 37 °C. EC_{50} values represent the concentration of the compound required to inhibit the HIV-1 infection by 50%. The data were obtained from three independent experiments by the NCK assay.

We next focused on the isothiazolopyrimidine scaffold of **2a** with a characteristic S–N covalent bond, which is contained in several anti-HIV agents against HIV-1 nucleocapsid protein 7 (NCp7).[22–24] We assessed the stability of compound **2a** under identical GSH-containing conditions (Fig. 4). In 10 mM GSH solution at 37 °C, compound **2a** was also immediately converted to a thiophenol derivative **4a** with potent anti-HIV activity (<3 min). The two-fold more potent pyrimidobenzothiazine **1d** or isothiazolopyrimidine **2d** was also converted under identical reductive conditions into the corresponding thiophenol derivative **4d**, which has similar anti-HIV activity to those of **1d** and **2d**.[25] The thiophenol derivative **4g**, which was obtained by conversion from the inactive pyrimidobenzothiazine **1g** or isothiazolopyrimidine **2g** under the GSH-mediated conditions, exhibited no anti-HIV activity. Thus, the anti-HIV activities of the PD 404182 derivatives (**1a**, **1d** and **1g**) and isothiazolopyrimidine derivatives (**2a**, **2d** and **2g**) corresponded, at least in part, to those of the thiophenol derivatives (**4a**, **4d** and **4g**). These results suggest that the tricyclic structures of **1a** and **2a** are the prodrug forms, which could be transformed into **4a** under intracellular conditions of high GSH concentrations in host cells. Interestingly, inactive analogues with scaffolds similar to PD 404182 (**1a**) or compound **2a** were not converted into thiophenol **4a** (Fig. 5). For example, compound **10**,[26] thioanisole derivative 7, benzo[4,5]thiazolo[3,2-*a*]pyrimidine **11** (the structural isomer of **2a**),[27] and saccharin-like derivative **12**[28] were completely stable under high concentrations of GSH for 24 hours. Therefore, the pyrimidobenzothiazine scaffold in **1a** and the isothiazolopyrimidine scaffold in **2a** structurally satisfied two criteria, which would make them good prodrugs of **4a**.

Taken together, the structure–activity relationships and antiviral profiles were similar between the PD 404182 derivatives **1** and benzo[4,5]isothiazolo[2,3-*a*]pyrimidine derivatives **2**. Under the reductive conditions corresponding to the intracellular environment, these scaffolds were efficiently converted to the common ring-opened thiophenol derivatives with potent anti-HIV activity. In addition, these two scaffolds inhibited not only HIV-1 infection at an early stage, but also several RNA and DNA viruses as we and others recently reported.[5–8,10,11] In light of these findings, it was suggested that PD 404182 and benzo-[4,5]isothiazolo[2,3-*a*]pyrimidine derivatives may achieve their antiviral activities by acting

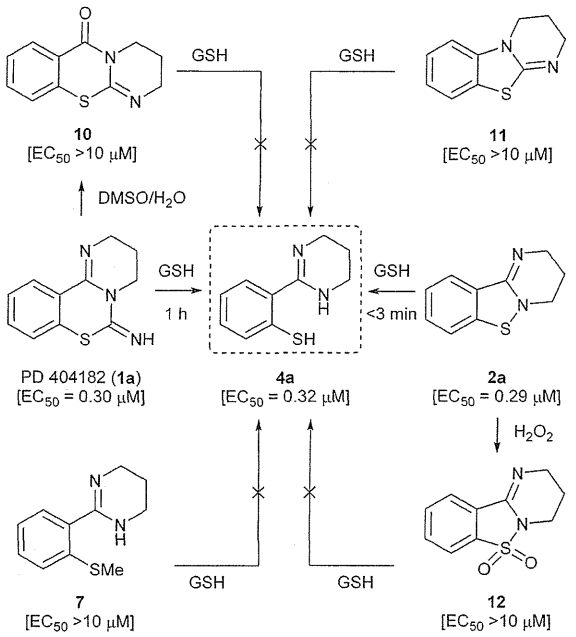

Fig. 5 Reactions of PD 404182, benzo[4,5]isothiazolo[2,3-*a*]pyrimidines and the inactive analogues under reductive conditions in the presence of GSH at 37 °C. EC_{50} values represent the concentration of the compound required to inhibit the HIV-1 infection by 50%. The data were obtained from three independent experiments by the NCK assay.

through an identical intermediate or *via* an interaction with a similar target molecule(s) or mechanism of action in an intracellular compartment. A viral target molecule(s) or mechanism (s) has not yet been determined,[14] but these heterocyclic compounds could conceivably regulate the defense mechanism(s) of the host cells.

Conclusions

We have unveiled the chemical transformations of pyrimido-[1,2-*c*][1,3]benzothiazin-6-imine and benzo[4,5]isothiazolo-[2,3-*a*]pyrimidine scaffolds, which yield compounds with potent antiviral activities. Under the reductive conditions meant to mimic intracellular GSH levels, the covalent S–N bond of the isothiazole substructure in **2a** was cleaved to provide the ring-opened 2-(2-mercaptophenyl)tetrahydropyrimidine **4a** with potent anti-HIV activity, which was also generated from PD 404182 (**1a**) under identical conditions. The similar structure–activity relationships and antiviral profiles between compounds **1a** and **2a** suggested that these could possibly be the prodrug forms for the common bioactive substance **4a** that binds with the potential target molecule(s) in host cells.

Experimental section

General

^{1}H NMR spectra were recorded using a JEOL ECA-500 spectrometer. Chemical shifts are reported in δ (ppm) relative to Me_4Si as an internal standard. ^{13}C NMR spectra were referenced to the residual solvent signal. Exact mass (HRMS) spectra were recorded on a JMS-HX/HX 110A mass spectrometer or Shimadzu LC-ESI-IT-TOF-MS equipment. For flash chromatography, Wakogel C-300E (Wako) and CHROMATOREX NH DM1080 (Fuji Silysia) were employed. For analytical HPLC, a Cosmosil 5C_{18}-ARII column (4.6 × 250 mm, Nacalai Tesque, Inc.) was employed with a linear gradient of CH_3CN containing 0.1% (v/v) aq. TFA at a flow rate of 1 cm^3 min^{-1}, and eluting products were detected by UV at 254 nm. Preparative HPLC was performed using a Cosmosil 5C_{18}-ARII preparative column (20 × 250 mm, Nacalai Tesque, Inc.) with a linear gradient of CH_3CN containing 0.1% (v/v) aq. TFA at a flow rate of 8 cm^3 min^{-1}. The purity of the compounds was determined as no less than 95% by combustion analysis or HPLC analysis. Preparation of the compounds **1–3**, **4d**, **6**, **8**, **13–15** was already reported from our laboratory.[7,8,11,15]

2-(2-Mercaptophenyl)-1,4,5,6-tetrahydropyrimidine (4a). Method A: TFA (3.70 cm^3, 50.0 mmol) was added to a suspension of PD 404182 (**1a**) (1.09 g, 5.00 mmol) in $CHCl_3$ (50.0 cm^3) and EtOH (75.0 cm^3) dropwise. After being stirred at room temperature for 1 h, the mixture was quenched with Et_3N (7.20 cm^3, 50.0 mmol) at 0 °C and was concentrated. The crude product was purified by flash chromatography over NH silica gel with $CHCl_3$–MeOH (10 : 0 to 9 : 1) to give the title compound **4a** as yellow crystals (999 mg, quant.); mp 208–210 °C (from *n*-hexane–$CHCl_3$–MeOH); IR (neat) ν_{max}/cm^{-1}: 3185–3092 (SH), 1590 (C=N); δ_H (500 MHz, CD_3OD): 2.05–2.09 (2H, m, CH_2), 3.55 (4H, t, J 5.7, CH_2), 6.87–6.91 (1H, m, Ar), 7.06 (1H, ddd, $J_1 = J_2$ 8.0, J_3 1.7, Ar), 7.28 (1H, dd, J_1 7.7, J_2 1.4, Ar), 7.56 (1H, dd, J_1 8.0, J_2 1.1, Ar); δ_C (125 MHz, DMSO-d_6): 18.1, 38.1 (2C), 118.7, 122.8, 126.7, 128.8, 137.8, 158.9, 159.8; HRMS (FAB): *m/z* calcd for $C_{10}H_{13}N_2S$ $[M + H]^+$ 193.0799; found: 193.0801.

Method B: 3,4-dihydro-2*H*,6*H*-pyrimido[1,2-*c*][1,3]benzothiazine-6-thione **3a**[15] (1.15 g, 4.90 mmol) was suspended in 0.1 N NaOH in MeOH–H_2O (9 : 1, 98.0 cm^3). After being stirred under reflux for 12 h, the mixture was quenched with 1 N HCl until pH was adjusted to 7. The whole mixture was extracted with $CHCl_3$–MeOH (95 : 5), and dried over $MgSO_4$. After concentration, the resulting solid was recrystallized from Et_2O–$CHCl_3$–MeOH to give the title compound **4a** as an yellow solid (655 mg, 70%): spectral data were in good agreement with those of the compound that was synthesized using method A.

2-(3-Bromo-2-mercaptophenyl)-1,4,5,6-tetrahydropyrimidine (4g). By using a procedure similar to that described for the preparation of the compound **4a** from **1a**, compound **1g**[7] (45.0 mg, 0.152 mmol) was converted to the title compound **4g** as a colorless solid (29.6 mg, 72%); mp 260–262 °C (from *n*-hexane–$CHCl_3$–MeOH); IR (neat) ν_{max}/cm^{-1}: 2895–2795 (SH), 1626 (C=N); δ_H (500 MHz, DMSO-d_6): 1.88–1.93 (2H, m, CH_2), 3.44 (4H, t, J 5.7, CH_2), 6.58 (1H, dd, $J_1 = J_2$ 7.7, Ar), 7.29 (1H, d, J 8.0, Ar), 7.53 (1H, d, J 8.0, Ar), 10.85 (2H, br s); δ_C (125 MHz, DMSO-d_6): 17.8, 38.2 (2C), 117.5, 126.2, 128.1, 132.8, 133.4, 160.1, 160.7; anal. calcd for

$C_{10}H_{11}BrN_2S$: C, 44.29; H, 4.09; N, 10.33. Found: C, 44.12; H, 4.08; N, 10.31.

2-[2-(Methylthio)phenyl]-1,4,5,6-tetrahydropyrimidine (7). 2-(Methylthio)benzaldehyde **5** (90% purity, 0.430 cm^3, 3.00 mmol) was reacted with propylenediamine (0.300 cm^3, 3.60 mmol), K_2CO_3 (1.24 g, 9.00 mmol) and I_2 (952 mg, 3.75 mmol). The crude compound was purified by flash chromatography over NH silica with $CHCl_3$–MeOH (10 : 0 to 10 : 1) followed by recrystallization from *n*-hexane–$CHCl_3$ to give the title compound **7** as colorless crystals (294 mg, 48%): mp 110–112 °C; IR (neat) ν_{max}/cm^{-1}: 1621 (C=N); δ_H (500 MHz, $CDCl_3$): 1.82–1.87 (2H, m, CH_2), 2.43 (3H, s, CH_3), 3.45 (4H, t, *J* 5.7, CH_2), 4.68 (1H, br s, NH), 7.12 (1H, ddd, J_1 = J_2 7.4, J_3 1.1, Ar), 7.20 (1H, d, *J* 6.9, Ar), 7.29 (1H, ddd, J_1 = J_2 7.6, J_3 1.5, Ar), 7.36 (dd, J_1 7.4, J_2 1.7, 1H, Ar); δ_C (125 MHz, $CDCl_3$): 16.0, 20.6, 42.1 (2C), 124.6, 125.5, 128.3, 129.1, 136.7, 137.0, 154.8; HRMS (ESI): *m/z* calcd for $C_{11}H_{15}N_2S$ $[M + H]^+$ 207.0956; found: 207.0954.

2-(2-Aminophenyl)-1,4,5,6-tetrahydropyrimidine (9). A mixture of 2-[2-*N*-(*p*-toluenesulfonylamino)phenyl]-1,4,5,6-tetrahydropyrimidine **8**[7] (494 mg, 1.50 mmol) in conc. H_2SO_4 (10.0 cm^3) was stirred at 100 °C for 30 min, the mixture was cooled to 0 °C, and then pH was adjusted to 12–14 with 2 N NaOH. The whole mixture was extracted with $CHCl_3$, and dried over $MgSO_4$. After concentration, the resulting solid was recrystallized from *n*-hexane–$CHCl_3$ to give the title compound **9** as colorless crystals (137 mg, 52%): mp 83–85 °C; IR (neat) ν_{max}/cm^{-1}: 2931 (NH_2), 2851 (NH_2), 1620 (C=N); δ_H (500 MHz, $CDCl_3$): 1.81–1.86 (2H, m, CH_2), 3.48 (4H, t, *J* 5.7, CH_2), 4.71 (1H, br s, NH), 5.72 (2H, br s, NH_2), 6.61–6.66 (2H, m, Ar), 7.07–7.10 (1H, m, Ar), 7.23–7.26 (1H, m, Ar); δ_C (125 MHz, $CDCl_3$): 20.7, 42.0 (2C), 116.56, 116.61, 119.3, 126.3, 129.9, 147.1, 155.1; anal. calcd for $C_{10}H_{14}N_3$: C, 68.54; H, 7.48; N, 23.98. Found: C, 68.28; H, 7.57; N, 23.75.

3,4-Dihydro-2*H*,6*H*-benzo[*e*]pyrimido[2,1-*b*][1,3]thiazin-6-one (10). PD 404182 (**1a**) (20.0 mg, 0.0920 mmol) in DMSO (0.920 cm^3) was dissolved in H_2O (92.0 cm^3). After being stirred at 37 °C for 26 h, the mixture was purified by HPLC. The resulting solid was dissolved in EtOAc, and washed with sat. $NaHCO_3$. The extract was dried over $MgSO_4$, and concentrated to give the title compound **10** as colorless crystals (5.2 mg, 27%); mp 132–134 °C (from toluene); IR (neat) ν_{max}/cm^{-1}: 1662 (C=O), 1608 (C=N); δ_H (500 MHz, $CDCl_3$): 1.98–2.03 (2H, m, CH_2), 3.57 (2H, t, *J* 5.7, CH_2), 4.02 (2H, t, *J* 6.0, CH_2), 7.17 (1H, d, *J* 8.0, Ar), 7.26–7.29 (1H, m, Ar), 7.47 (1H, ddd, J_1 = J_2 7.7, J_3 1.6, Ar), 8.24 (1H, dd, J_1 8.0, J_2 1.1, Ar); δ_C (125 MHz, $CDCl_3$): 21.1, 42.3, 46.1, 122.7, 124.0, 126.0, 131.0, 133.2, 134.3, 147.0, 161.7; HRMS (FAB): *m/z* calcd for $C_{11}H_{11}N_2OS$ $[M + H]^+$ 219.0592; found: 219.0584. Spectral data were in good agreement with those previously reported.[26]

Crystal structure: $C_{11}H_{10}N_2OS$, M_w: 218.27, primitive monoclinic, a = 10.7456(6), b = 10.9466(6), c = 16.6473(7) Å, β = 97.422(2)°, V = 1941.78(17) $Å^3$, space group $P2_1/n$ (no. 14), Z = 8. The data were collected with a Rigaku R-AXIS RAPID diffractometer using graphite monochromated Mo-Kα radiation at −93 K. 18 534 Reflections were measured, 4420 unique (R_{int} = 0.0220) which were used in all calculations. The final wR was 0.0796. The substance was crystallized from toluene. The CCDC deposition number: 1037500.

3,4-Dihydro-2*H*-benzo[4,5]thiazolo[3,2-*a*]pyrimidine (11). Following the reported procedure,[27] 2-chloro-1,3-benzothiazole (0.619 cm^3, 5.00 mmol) was converted to the title compound **11**, as a pale yellow solid (407 mg, 2 steps 73%), by the reaction with 3-amino-1-propanol (0.381 cm^3, 5.00 mmol). The product (80.8 mg) was purified by HPLC to give the compound **11** as a colorless solid (72.3 mg, TFA salt): IR (neat) ν_{max}/cm^{-1}: 3274–3181 (OH), 1672 (C=O), 1632 (C=N); δ_H (500 MHz, CD_3OD): 2.31–2.36 (2H, m, CH_2), 3.70 (2H, t, *J* 5.7, CH_2), 4.27 (2H, t, *J* 6.0, CH_2), 7.42–7.45 (1H, m, Ar), 7.57–7.61 (2H, m, Ar), 7.84 (1H, d, *J* 8.0, Ar); δ_C (125 MHz, CD_3OD): 19.2, 41.3, 44.0, 113.5, 118.0 (q, *J* 291.5), 123.1, 124.1, 126.7, 129.2, 140.0, 162.4 (q, *J* 36.0), 166.0; HRMS (FAB): *m/z* calcd for $C_{10}H_{11}N_2S$ $[M + H]^+$ 191.0643; found: 191.0641.

3,4-Dihydro-2*H*-benzo[4,5]isothiazolo[2,3-*a*]pyrimidine 6,6-dioxide (12). 50% H_2O_2 (0.0391 cm^3, 0.638 mmol) was added to a suspension of compound **2a** (48.5 mg, 0.159 mmol, TFA salt) in TFA (0.610 cm^3) dropwise. After being stirred at room temperature for 24 h, the mixture was quenched with Et_3N (1.50 cm^3), and the whole mixture was extracted with EtOAc. The extract was washed with sat. $NaHCO_3$, brine, and dried over $MgSO_4$. After concentration, the residue was purified by flash chromatography over aluminum oxide with *n*-hexane–EtOAc (3 : 2 to 1 : 1) to give the title compound **12** as colorless crystals (25.2 mg, 71%): mp 146–148 °C (from Et_2O–MeOH); IR (neat) ν_{max}/cm^{-1}: 1670 (C=N); δ_H (500 MHz, $CDCl_3$): 2.01–2.05 (2H, m, CH_2), 3.70 (2H, t, *J* 5.7, CH_2), 3.79 (2H, t, *J* 6.0, CH_2), 7.70–7.76 (2H, m, Ar), 7.85–7.88 (1H, m, Ar), 7.98–8.01 (1H, m, Ar); δ_C (125 MHz, $CDCl_3$): 19.5, 36.5, 44.2, 120.7, 122.8, 129.6, 132.4, 133.6, 134.8, 142.7; anal. calcd for $C_{10}H_{10}N_2O_2S$: C, 54.04; H, 4.54; N, 12.60. Found: C, 53.89; H, 4.74; N, 12.36.

2-(2-Hydroxyphenyl)-1,4,5,6-tetrahydropyrimidine (16).[21] A mixture of methyl salicylate (1.29 cm^3, 10.0 mmol) and propylenediamine (2.56 cm^3, 30.0 mmol) was refluxed for 16 h. The crude product was dissolved in MeOH, and crystallized with Et_2O. The precipitate was filtered, and the unreacted propylenediamine was removed by washing with Et_2O. The resulting solid was purified by flash chromatography over aluminum oxide with $CHCl_3$–MeOH (10 : 0 to 10 : 1) to give the title compound **16** as colorless crystals (497 mg, 28%): mp 259–261 °C (from Et_2O–MeOH); IR (neat) ν_{max}/cm^{-1}: 3212–3050 (OH), 1620 (C=N); δ_H (500 MHz, DMSO-d_6): 1.83–1.88 (2H, m, CH_2), 3.40 (4H, t, *J* 5.7, CH_2), 6.27–6.30 (1H, m, Ar), 6.46 (1H, d, *J* 8.6, Ar), 7.04–7.08 (1H, m, Ar), 7.45 (1H, dd, J_1 8.0, J_2 1.7, Ar), 12.10 (1H, br s, OH); δ_C (125 MHz, CD_3OD): 20.0, 39.3 (2C), 111.2, 114.5, 124.4, 126.3, 135.1, 160.9, 172.5; anal. calcd for $C_{10}H_{12}N_2O$: C, 68.16; H, 6.86; N, 15.90. Found: C, 68.13; H, 7.03; N, 16.09.

Determination of anti-HIV activity

The anti-HIV activity of a series of compounds against HIV-1_{IIIB} was determined by the NCK assay.[29] The target

cells (NCK45-β-Gal; 10^4 cells per well) were plated in 96-well flat microtiter culture plates. On the following day, the cells were inoculated with HIV-1 (60 NCK U per well, giving 60 blue cells after 48 h of incubation) and cultured in the presence of various concentrations of the test compounds in fresh medium. Forty-eight hours after viral exposure, all the blue cells stained with X-Gal (5-bromo-4-chloro-3-indolyl-β-D-galactopyranoside) were counted in each well. Cytotoxic effects were not observed at 10 μM except for compound **2g**.

The activity of test compounds was determined as the concentration that blocked HIV-1 infection by 50% (50% effective concentration [EC_{50}]). EC_{50} was determined by using the following formula:

$$EC_{50} = 10^{[\log(A/B)\times(50-C)/(D-C)+\log(B)]},$$

where *A*, of the two points on the graph that bracket 50% inhibition, the higher concentration of the test compound; *B*, of the two points on the graph that bracket 50% inhibition, the lower concentration of the test compound; *C*, inhibitory activity (%) at the concentration *B*; *D*, inhibitory activity (%) at the concentration *A*.

Glutathione-mediated transformation of pyrimidobenzothiazine and isothiazolopyrimidine derivatives

The compound (1 mM) was incubated in 10 mM GSH (in a mixture of 50 mM phosphate buffer (pH 7.4) and MeCN [75 : 25 (v/v) or 1 : 1 (v/v)]) at 37 °C. The sample was analyzed by HPLC and the peak area was recorded by UV detection at 254 nm. The concentrations of the products were calculated using previously determined calibration curves. Of note, the GSH-mediated transformation from **1a** was slightly accelerated by the addition of MeCN in phosphate buffer.

Acknowledgements

This work was supported by Grants-in-Aid for Scientific Research from JSPS, Japan; Platform for Drug Discovery, Informatics, and Structural Life Science from MEXT, Japan; a Grant-in-Aid for Research on HIV/AIDS from the Ministry of Health and Welfare of Japan. T.M. is grateful for JSPS Research Fellowships for Young Scientists.

References

1 PD 404182 (**1a**) was previously reported to be an enzyme inhibitor against 3-deoxy-D-*manno*-octulosonic acid 8-phosphate synthase[2] and phosphopantetheinyl transferase.[3] In addition, it was recently reported that PD 404182 (**1a**) inhibits human dimethylarginine dimethylaminohydrolase isoform 1 (DDAH).[4]

2 M. R. Birck, T. P. Holler and R. W. Woodard, *J. Am. Chem. Soc.*, 2000, **122**, 9334–9335.

3 C. R. Vickery, N. M. Kosa, E. P. Casavant, S. Duan, J. P. Noel and M. D. Burkart, *ACS Chem. Biol.*, 2014, **9**, 1939–1944.

4 Y. T. Ghebremariam, D. A. Erlanson and J. P. Cooke, *J. Pharmacol. Exp. Ther.*, 2014, **348**, 69–76.

5 K. Chockalingam, R. L. Simeon, C. M. Rice and Z. Chen, *Proc. Natl. Acad. Sci. U. S. A.*, 2010, **107**, 3764–3769.

6 A. M. Chamoun, K. Chockalingam, M. Bobardt, R. Simeon, J. Chang, P. Gallay and Z. Chen, *Antimicrob. Agents Chemother.*, 2012, **56**, 672–681.

7 T. Mizuhara, S. Oishi, H. Ohno, K. Shimura, M. Matsuoka and N. Fujii, *Org. Biomol. Chem.*, 2012, **10**, 6792–6802.

8 T. Mizuhara, S. Oishi, H. Ohno, K. Shimura, M. Matsuoka and N. Fujii, *Bioorg. Med. Chem.*, 2012, **20**, 6434–6441.

9 T. Mizuhara, S. Oishi, H. Ohno, K. Shimura, M. Matsuoka and N. Fujii, *Bioorg. Med. Chem.*, 2013, **21**, 2079–2087.

10 A. M. Chamoun-Emanuelli, M. Bobardt, B. Moncla, M. K. Mankowski, R. G. Ptak, P. Gallay and Z. Chen, *Antimicrob. Agents Chemother.*, 2014, **58**, 687–697.

11 S. Okazaki, T. Mizuhara, K. Shimura, H. Murayama, H. Ohno, S. Oishi, M. Matsuoka and N. Fujii, *Bioorg. Med. Chem.*, 2015, **23**, 1447–1452.

12 M. Baba, D. Schols, R. Pauwels, H. Nakashima and E. De Clercq, *J. Acquired Immune Defic. Syndr.*, 1990, **3**, 493–499.

13 T. Matthews, M. Salgo, M. Greenberg, J. Chung, R. DeMasi and D. Bolognesi, *Nat. Rev. Drug Discovery*, 2004, **3**, 215–225.

14 Of note, it was reported that PD 404182 showed the antiviral activities by the virucidal effect *via* the physical disruption of virions, see ref. 6 and 10.

15 T. Mizuhara, S. Oishi, N. Fujii and H. Ohno, *J. Org. Chem.*, 2010, **75**, 265–268.

16 M. Ishihara and H. Togo, *Tetrahedron*, 2007, **63**, 1474–1480.

17 For a review on the function of glutathione, see: R. Franco, O. J. Schoneveld, A. Pappa and M. I. Panayiotidis, *Arch. Physiol. Biochem.*, 2007, **113**, 234–258 and references cited therein.

18 Compound **4a** was also identified from HTS as an antibacterial agent that inhibits localization of lipoproteins (Lol) during cell wall biosynthesis, see: H. Ito, A. Ura, Y. Oyamada, H. Yoshida, J. Yamagishi, S. Narita, S. Matsuyama and H. Tokuda, *Microbiol. Immunol.*, 2007, **51**, 263–270.

19 During the course of our investigations, an initial report describing GSH-mediated degradation of PD 404182 appeared, see ref. 4.

20 In the absence of GSH, compound **1a** was converted into pyrimidothiazinone **10** as discussed above.

21 R. Mitsuhashi, T. Suzuki and Y. Sunatsuki, *Inorg. Chem.*, 2013, **52**, 10183–10190.

22 J. A. Loo, T. P. Holler, J. Sanchez, R. Gogliotti, L. Maloney and M. D. Reily, *J. Med. Chem.*, 1996, **39**, 4313–4320.

23 T. Vercruysse, B. Basta, W. Dehaen, N. Humbert, J. Balzarini, F. Debaene, S. Sanglier-Cianférani,

C. Pannecouque, Y. Mély and D. Daelemans, *Retrovirology*, 2012, **9**, 95–108.
24 C. Pannecouque, B. Szafarowicz, N. Volkova, V. Bakulev, W. Dehaen, Y. Mély and D. Daelemans, *Antimicrob. Agents Chemother.*, 2010, **54**, 1461–1468.
25 The transformations from **1f** and **2f** into the ring-opened thiophenol derivative were also observed in the presence of GSH.
26 D. Chen, J. Wu, J. Yang, L. Huang, Y. Xiang and W. Bao, *Tetrahedron Lett.*, 2012, **53**, 7104–7107.
27 P. A. Woods, L. C. Morrill, T. Lebl, A. M. Z. Slawin, R. A. Bragg and A. D. Smith, *Org. Lett.*, 2010, **12**, 2660–2663.
28 S. Sivaramakrishnan, A. H. Cummings and K. S. Gates, *Bioorg. Med. Chem. Lett.*, 2010, **20**, 444–447.
29 K. Kajiwara, E. Kodama, Y. Sakagami, T. Naito and M. Matsuoka, *J. Clin. Microbiol.*, 2008, **46**, 792–795.

Passive transfer of neutralizing mAb KD-247 reduces plasma viral load in patients chronically infected with HIV-1

Shuzo Matsushita[a], Kazuhisa Yoshimura[a,b], Kristel Paola Ramirez[a], Jaya Pisupati[c], Toshio Murakami[d], on behalf of the KD-1002 Study Group

Objective: Neutralizing antibodies against HIV-1 such as a humanized mAb KD-247 can mediate effector functions that attack infected cells *in vitro*. However, the clinical efficacy of neutralizing antibodies in infected individuals remains to be determined. We evaluated the safety, tolerability and pharmacokinetics of KD-247 infusion and its effect on plasma HIV-1 RNA load and $CD4^+$ T-cell count.

Design and methods: KD-1002 is a phase Ib, double-blind, placebo-controlled, dose-escalation study of KD-247 in asymptomatic HIV-1 seropositive individuals who did not need antiretroviral therapy. Individuals were randomized to 4, 8 or 16 mg/kg KD-247 or placebo, and received three infusions over a 2-week period.

Results: Patients were randomized to receive one of the three doses of KD-247 and the treatment was well tolerated. We observed a significant decrease in HIV RNA in the 8 and 16 mg/kg KD-247 cohorts, with two individuals who achieved more than 1 log reduction of HIV RNA. Two patients in the 16 mg/kg cohort had selections and/or mutations in the V3-tip region that suggested evasion of neutralization. Long-term suppression of viral load was observed in one patient despite a significant decrease in plasma concentration of KD-247, suggesting effects of the antibody other than neutralization or loss of fitness of the evading virus.

Conclusion: The results indicate that KD-247 reduces viral load in patients with chronic HIV-1 infection and further clinical trials are warranted.

AIDS 2015, **29**:453–462

Keywords: antibody-dependent cell cytotoxicity, escape mutations, HIV-1, mAb, neutralizing antibody, passive immunization

Introduction

Despite the significant reduction in morbidity and mortality following combination antiretroviral therapy (cART), there is emerging evidence that people with successfully treated HIV-1 infection age prematurely, leading to progressive multiorgan diseases referred to as comorbidity. The pathogenic process has been associated with long-term use of antiviral drugs, residual viral production and subsequent chronic inflammation [1]. In contrast to the current cART that only targets viral replication, neutralizing or nonneutralizing antibodies against HIV-1 can mediate effector functions that attack infected cells *in vitro* [2,3]. However, the clinical efficacy

[a]Center for AIDS Research, Kumamoto University, Kumamoto, [b]AIDS Research Center, National Institute of Infectious Diseases, Tokyo, Japan, [c]Quintiles Inc., Overland Park, Kansas, USA, and [d]The Chemo-Sero-Therapeutic Research Institute (Kaketsuken), Kumamoto, Japan.

Correspondence to Shuzo Matsushita, Center for AIDS Research, Kumamoto University, 2-2-1 Honjo, Chyuo-ku, Kumamoto 860-0811, Japan.

Tel: +81 96 373 6536; fax: +81 96 373 6537; e-mail: shuzo@kumamoto-u.ac.jp

Received: 12 August 2014; revised: 16 December 2014; accepted: 17 December 2014.

DOI:10.1097/QAD.0000000000000570

ISSN 0269-9370

of neutralizing antibodies in infected individuals remains to be determined.

Previous studies revealed that human antibodies to HIV-1 can neutralize a broad range of viral isolates *in vitro* and protect nonhuman primates against infection [4–6]. Effective control of HIV-1 by combinations of broadly neutralizing antibody (bnAb) in chronically infected humanized mice and simian–human immunodeficiency virus (SHIV)-infected macaques have been reported [7–9]. However, previous human studies concluded that treatment with neutralizing antibodies had only limited effects against established HIV-1 infection [10,11].

Here, we report the results of a phase Ib dose-escalation study of a neutralizing mAb, KD-247 (international nonproprietary name: suvizumab) in asymptomatic HIV-1 seropositive individuals who did not at the time need cART. The epitope recognized by the mAb was mapped to IGPGR at the tip of the third variable loop of HIV-1 gp120 (V3-tip) that covers about half of HIV-1 in subtype B [12,13]. KD-247 belongs to the antibodies that have limited breadth and potency in standard neutralization assays as compared with bnAbs [14]. However, passive transfer of KD-247 may have an impact on patients infected with HIV-1 that matches for KD-247 binding.

The objectives of this phase Ib study were to evaluate the safety and tolerability of three infusions of KD-247 over 2 weeks in HIV-1 seropositive individuals, to determine the pharmacokinetic parameters and to assess the effect of KD-247 infusions on plasma HIV-1 RNA load and $CD4^+$ T-cell counts.

Materials and methods

Protein-based KD-247 binding test

The binding activity of KD-247 to recombinant proteins that expressed the V3 region was examined prior to the phase Ib study. The gene containing the V3 region in viruses extracted from patients' plasma or peripheral blood mononuclear cells (PBMCs) was amplified by a nested PCR method using first primers, 5′-ACACATG GAATTAGGCCAGT-3′ (OA-4) and 5′-AAATTCCC CTCCACAATTAA-3′ (OD-4), and second primers, 5′-GCCGGATCCTCAACTCAACTGCTGTTAAAT-3′ (EB-2) and 5′-GCTCTGCAGTCAAATTTCTGGGT CCCCTCCTGAGG-3′ (EC-2). After the purification of the amplified DNA, this segment was cleaved and inserted into a vector plasmid containing β-galactosidase (β-Gal). Separately, each cloned *Escherichia coli* with its gene sequence analysed was cultured, and the recombinant fusion protein derived from the V3 region and β-Gal (V3-Gal) was obtained. An ELISA was performed to normalize the V3-Gal concentration. The expressed V3-Gal or commercially available β-Gal (CN Bioscience, La Jolla, California, USA) as a reference standard was added to a 96-well ELISA plate immobilized with the β-Gal antibody (Chemicon International, Temecula, California, USA). Peroxidase-labelled β-Gal antibody (Rockland Immunochemicals, Limerick, Pennsylvania, USA) was used as a detecting antibody. To evaluate the reactivity of KD-247 to each V3-Gal protein, 200 ng/ml of V3-Gal was captured on a plate coated with the β-Gal antibody, followed by incubation with KD-247 (1 μg/ml) and the reactivity was detected by the peroxidase-labelled anti-human IgG antibody.

KD-1002 clinical trial

KD-1002 was a phase I, double-blind, placebo-controlled, dose-escalation, cohort study of KD-247 in asymptomatic HIV-1 seropositive individuals who did not currently need ART. The study was conducted by investigators (who enrolled patients) at 15 study centres in the USA. Eligible patients were randomized to one of three doses of KD-247 (4, 8 or 16 mg/kg) or placebo (physiological saline), and received three infusions over a 2-week period (days 1, 8 and 15). A minimum of six active and three placebo patients for each dose cohort had to complete 2 weeks of infusions. Patients in all three cohorts were followed for 12–16 weeks after the final infusion of study drug. Dose escalation could proceed only after review of the safety data up to Day 18 for all patients in the lower-dose cohort.

In addition to usual entry criteria, patients were considered eligible for participation in the study if they were asymptomatic HIV-1 seropositive individuals who at the time of study did not need ART; demonstrated an HIV-1 RNA copy number of 1000–100 000 and $CD4^+$ T-cell count more than 350 cells/μl; and who by genotyping had a sequence of the portion of the HIV envelope gene encoding the principal neutralizing determinant that is consistent with neutralization by KD-247. Plasma HIV-1 RNA samples were measured using the Roche Amplicor HIV-1 RNA assay (standard) with a dynamic range of 400–750 000 copies/ml and the Roche Amplicor Ultrasensitive plasma HIV-1 RNA assay (ultrasensitive) with a dynamic range of 50–100 000 copies/ml (Roche Diagnostic Systems, Branchburg, New Jersey, USA). The $CD4^+$ and $CD8^+$ cell counts were measured using a flow cytometer (BD FACSCanto II; BD Biosciences, Franklin Lakes, New Jersey, USA). Potential switches of coreceptor use were monitored for the 8 and 16 mg/kg cohorts by the Trofile assay (Monogram Biosciences, San Francisco, California, USA), which uses the complete gp160 coding region of the HIV-1 envelope protein.

Genotypic screening for the clinical study was performed by SRL Medisearch Inc. (Tokyo, Japan). The gene containing the V3 region in viruses extracted from patients' plasma was amplified by a nested PCR method using first primers (OA-4 and OD-4) and second primers

(EB-2 and EC-2). After purification of the amplified DNA, this segment was cloned and sequenced to determine the gene containing the V3 region. Patients were screened by V3-tip amino acid sequences deduced from the results of genotypic analyses and judged as suitable for KD-247 treatment if all 10 viral clones conformed to the reference sequences. Six sequences of V3-tip that had a GPGR sequence and high binding activity to KD-247 (XIGPGRAL, XIGPGRSF, XIGPGRTF, XIGPGRAI, XIGPGRAF and XVGPGRAL; X was not K, P and R) were selected as the reference sequences for the genotyping test (Fig. 1a and b).

The study protocol and all amendments, written study patient information, informed consent form and any other appropriate study-related information were reviewed and approved by an independent ethics committee or institutional review board at each study centre. The study was conducted in accordance with Good Clinical Practice as required by the International Conference on Harmonisation guidelines and in accordance with country-specific and/or local laws and regulations governing clinical studies of investigational products. Compliance with these requirements also constituted conformity with the ethical principles of the Declaration of Helsinki. Prior to initiation of any study procedures, an informed consent agreement explaining the procedures of the study, together with the potential risk, was read by and explained to all patients.

The trial was registered at the ClinicalTrial.gov (National Library of Medicine at the National Institutes of Health) database with the registration number NCT00917813.

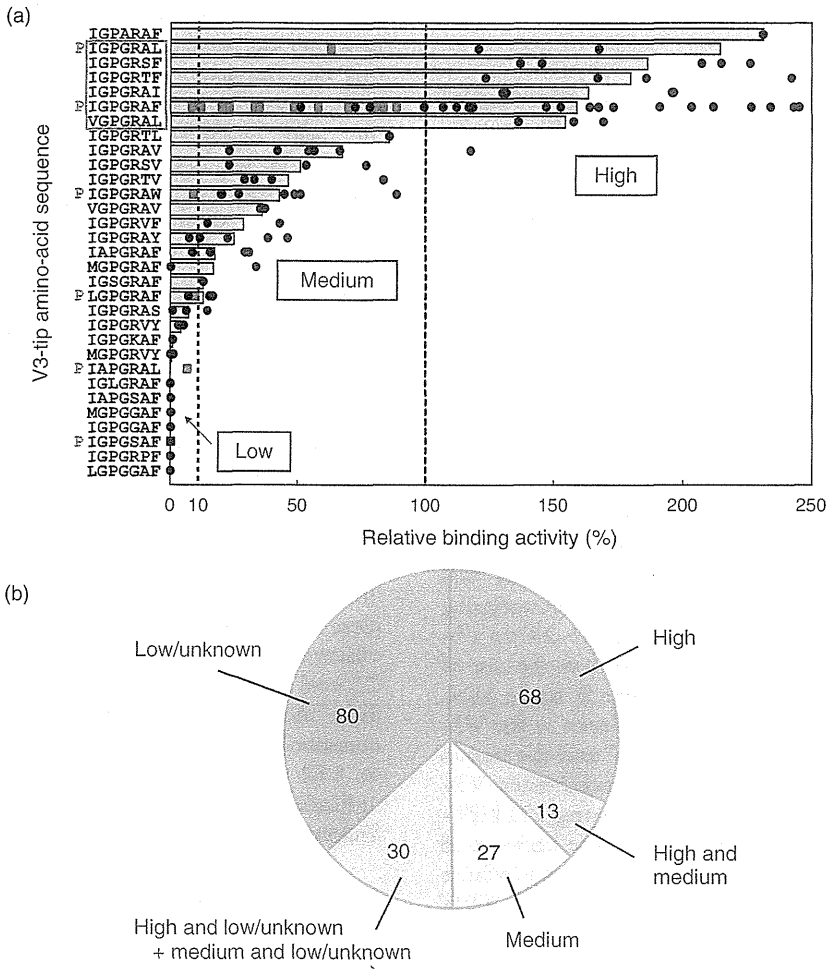

Fig. 1. Determination of reference sequences by a protein-based KD-247 binding test. (a) The binding of KD-247 to the recombinant fusion protein derived from the V3 region of HIV-1 gp120 and β galactosidase (V3-Gal) was indicated as relative activity of 100% in the case of the V3 sequence from the MN strain. The amino acid sequences of the V3-tip region in the viral clones whose mean relative KD-247 binding activity exceeded 100% were IGPARAF, IGPGRSF, IGPGRAL, IGPGRTF, IGPGRAI, VGPGRAL, and IGPGRAF. Above 100%, 10–100%, and <10% of binding activity was categorized as high, medium, and low, respectively. (b) Frequency of estimated KD-247 binding abilities using the 218 data from screened patients is shown. All 10 viral clones derived from 68 patients were estimated as high binding activity.

Pharmacokinetic analysis

Serum concentrations of KD-247 in pharmacokinetic samples were determined by ELISA using an antigen peptide [15]. The lower limit of quantitation for KD-247 was 0.2 μg/ml. Similarly, the two samples that were collected from the infusion bag were analysed for KD-247 concentration and reported as two individual concentrations. The average of the two concentrations was used for the calculation of actual total dose infused. Pharmacokinetic parameters for KD-247 were calculated from serum concentrations of the antibody by compartmental and noncompartmental methods. Actual sampling times were used for the computation of pharmacokinetic parameters. All pharmacokinetic calculations were performed using WinNonlin Professional version 5.2 (Pharsight Corp., Mountain View, California, USA) or SAS version 9.2 (SAS Institute, Cary, North Carolina, USA) or NONMEM version 6.0 (Certara USA, Inc., Princeton, New Jersey, USA).

Statistical analyses

Analyses of independent virological and immunological data were performed by two-tailed Mann–Whitney *U* tests. Statistical differences among groups were determined by performing one-way analysis of variance or the Kruskal–Wallis test with Dunn multiple comparison posthoc test. *P* value less than 0.05 was considered significant. Statistical analysis was performed using GraphPad Prism (GraphPad Software, Inc., La Jolla, California, USA).

Results

Determination of reference sequences

Prior to the phase Ib study, the binding activity of KD-247 to a protein that expressed the V3 region was evaluated, and patient selection criteria by genotyping were established (Fig. 1a). The binding of KD-247 to V3-Gal was indicated as relative activity of 100% in the case of the V3 sequence derived from a subtype B strain MN, which had the subtype B consensus sequence at the V3-tip. Relative binding activities of KD-247 and the amino acid sequence of the V3-tip of the recombinant V3-region expressing proteins were analysed using 122 HIV-1 clones derived from plasma or PBMCs. The amino acid sequences of the V3-tip region in the viral clones whose mean relative KD-247 binding activity exceeded 100% were IGPARAF, IGPGRSF, IGPGRAL, IGPGRTF, IGPGRAI, VGPGRAL and IGPGRAF, although the number of IGPARAF was only one. Most of the results using the recombinant V3 protein were in accord with the results using the short peptides by Pepscan [12]. However, a proline residue at the amino terminal of the V3-tip sequence markedly decreased the binding activity of KD-247 (Fig. 1a, red squares). The value bar of this graph indicates the mean binding activity, except for V3-Gal wherein there was a proline residue at the amino terminus. Considering the results of the examinations using V3-Gal and short peptides, and the consensus sequence of the subtype B virus, six sequences that had GPGR sequences and high binding activity to KD-247 (XIGPGRAL, XIGPGRSF, XIGPGRTF, XIGPGRAI, XIGPGRAF and XVGPGRAL; X was not K, P and R) were selected as the reference sequences of genotyping on the phase Ib clinical study.

Individual disposition

For the genotyping test for suitability, all 10 clones amplified from plasma RNA from 68 patients out of 218 matched the reference sequences corresponding to the high binding activity to KD-247 (Fig. 1b). A total of 295 patients were screened and 30 from the population with high binding activity were randomized and received study treatment, with seven receiving 4 mg/kg KD-247, six receiving 8 mg/kg KD-247, seven receiving 16 mg/kg KD-247 and 10 receiving placebo. Twenty-eight patients (93.3%) completed the study. There were no imbalances in the patient demographics that were expected to affect the data or interpretation of the results. Patient disposition and demographic and baseline information are summarized in Table 1 and Supplementary Table 1, http://links.lww.com/QAD/A629.

Safety and pharmacokinetic analysis

In general, KD-247 was well tolerated. There was no evidence of allergic or hypersensitivity reactions. Although the number of patients in each cohort was small, there was no evidence to support any hepatic, renal or cardiac toxicity. Supplementary Fig. 1, http://links.lww.com/QAD/A629 shows the phramacokinetic profiles of KD-247 for Day 1 following Infusion 1 and up to Day 99 following Infusion 3 on Day 15. All patients had concentrations above the lower limit of quantification (0.2 μg/ml) on Day 99. Dose proportionality across the dose range of 4–16 mg/kg for both Day 1 and Day 15 was observed. The systemic clearance varied from 18.3 to 22.9 ml/h, indicating that KD-247 was cleared slowly from the central compartment. Accumulation ratio as measured by Day 15/Day 1 exposure varied from 1.41 to 1.61 for C_{max} and from 1.67 to 1.78 for $AUC_{(0-\tau)}$, indicating that there was some accumulation of KD-247 following three infusions.

Effect of KD-247 infusions on plasma HIV-1 RNA load and $CD4^+$ T-cell counts

There was a trend towards moderate increase in $CD4^+$ and $CD8^+$ counts across dose cohorts (Supplementary Fig. 2a and b, http://links.lww.com/QAD/A629). The counts were not significantly higher than those for placebo. The changes in log-transformed plasma HIV-1 RNA from baseline in each cohort after Infusion 1 (a, Day 1), 2 (b, Day 8) and 3 (c, Day 15) are shown in Fig. 2. The impact of Infusion 1 was not evident for the viral load

Table 1. Patient demographics and baseline information.

Characteristic	Statistics	Patient group: Placebo ($n=10$)	KD-247 4 mg/kg ($n=7$)	KD-247 8 mg/kg ($n=6$)	KD-247 16 mg/kg ($n=7$)	Total ($n=30$)
Sex						
Percentage male	*n* (%)	90.0%	100%	100%	85.7%	93.3%
Age (years)	Mean	36.7	38.6	35.8	43.4	38.5
	SD	11.9	8.8	8.1	13.0	10.7
Weight (kg)	Mean	81.45	86.29	88.40	74.33	82.31
	SD	12.72	19.19	14.44	11.79	14.77
BMI (kg/m^2)	Mean	26.156	28.097	28.932	24.837	26.856
	SD	2.330	6.725	3.668	1.762	4.052
HIV-1 RNA (copies/ml)	Mean	15093	20226	20797	49729	25513
	SD	14404	17020	25059	28603	24335
CD4$^+$ cell count (cells/μl)	Mean	690	405	426	424	509
	SD	293	155	51	151	232
CD8$^+$ cell count (cells/μl)	Mean	823	1113	932	848	918
	SD	277	436	290	338	339
Coreceptor use[a]	R5 cases/total	6/6	NT[b]	3/5	4/5	13/16

CCR5, chemokine CC receptor 5; SD, standard deviation.
[a]Coreceptor use of plasma viruses was monitored for the 8 and 16 mg/kg cohorts by Trofile assay and expressed numbers of CCR5 use (R5) in total cases.
[b]Not tested.

reduction, and changes in plasma RNA were comparable to those in the placebo cohort in many cases (Fig. 2a). However, a moderate decrease in HIV-1 RNA was observed in the 8 and 16 mg/kg cohorts after Infusion 2, and three of six cases in the 8 mg/kg cohort and four of seven cases in the 16 mg/kg cohort showed a reduction greater than the average ± standard deviation (SD) of the placebo cohort (Fig. 2b). There was a significant reduction in HIV-1 RNA in the 8 and 16 mg/kg cohorts after Infusion 3, and five of six cases in the 8 mg/kg cohort and five of six cases in the 16 mg/kg cohort showed a reduction greater than the average ± SD of the placebo cohort (Fig. 2c). Longitudinal follow-up of HIV-1 RNA loads and log-transformed changes from baseline for each patient in all cohorts are summarized in Supplementary Table 2, http://links.lww.com/QAD/A629. The time points at which we detected a significant reduction of HIV-1 RNA load over the placebo cohort are shown in Fig. 2d and summarized in Supplementary Table 3, http://links.lww.com/QAD/A629. The changes in log-transformed plasma HIV-1 RNA from baseline in each cohort throughout the trial are shown in Fig. 2e, with additional time points that had a significant reduction in viral load. The dose proportional reduction of viral load continued for nearly 29 days, and thereafter, the level of suppression decreased with the plasma concentration of KD-247 (Fig. 2e). Although the mean profiles showed moderate decreases in viral RNA, the impact of KD-247 on individual cases was noteworthy. Among these, Case #03017 on Day 8 and Case #12044 on Day 16 achieved more than 1 $\log_{10}$ copies/ml reduction in HIV-1 RNA. The emergence of neutralization escape mutation (R315K) was observed on Day 22 for both cases (Table 2).

To clarify the impact of KD-247 on the reduction of plasma viral load, we analysed longitudinal changes in plasma concentration of KD-247 with HIV-1 RNA for the 16 mg/kg cohort (Fig. 3). We observed a reduction of HIV-1 RNA and viral-load set points in four of six cases. Case #10012 (Fig. 3a) was a typical case in which the reduction of plasma viral load was not seen on Day 1. However, reduction of HIV-1 RNA was observed at the predose of Infusion 2 on Day 8, and a further decrease was observed at Day 15. The plasma viral load remained at a lower level than baseline. Escape mutants for KD-247 were not found in this case. In contrast, Case #03017 (Fig. 3b) followed a different clinical course. Plasma viral load suppression was observed immediately after Infusion 1 and the effect persisted on Days 8 and 15. However, viral rebound was detected owing to the emergence of the neutralization escape mutants with R315K on Day 22. Case #12044 was remarkable in that the suppression of plasma viral load was observed at the predose of Infusion 2 on Day 8, and continued on Day 99 when the plasma concentration of KD-247 decreased to the lower level (Fig. 3c). We detected emergence of R315K mutation at a low frequency (1 in 10 clones) on Day 22, but the mutant was not found on Day 99 (Table 2). These results suggest that a sustained level of KD-247 blood concentration may not be necessary to control the viral load in blood.

We observed moderate suppression of plasma viral load in Case #01037 (Fig. 3d), especially after Infusion 3 on Day 15. Although the effect was marginal, the suppression persisted long after the final infusion. Viral load reduction by KD-247 was not evident for Cases #15017 and #01034 (Fig. 3e and f, respectively), although temporal suppression was observed after Infusion 3 on Day 15. The

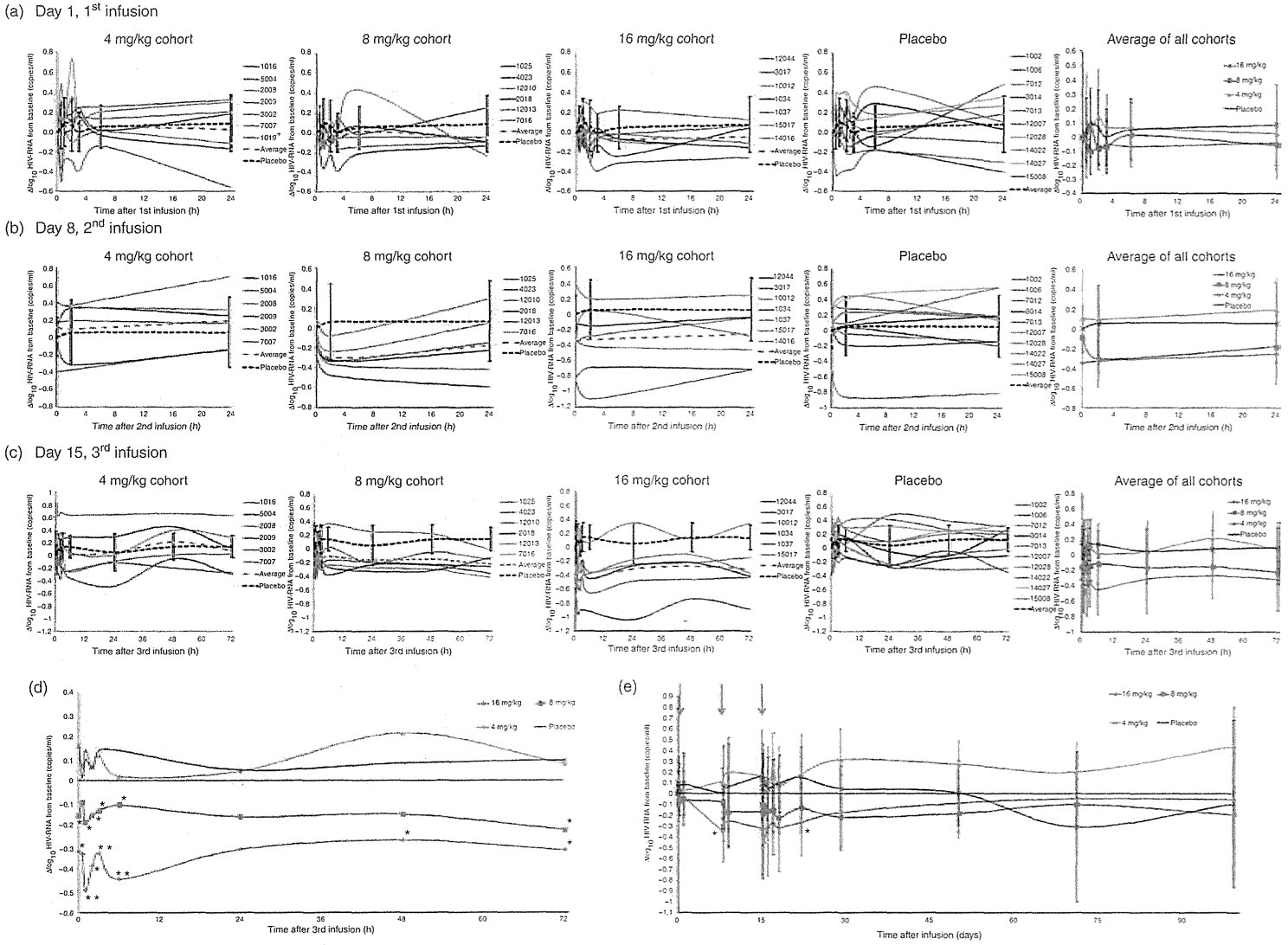

Fig. 2. Impact of three infusions of KD-247 on plasma HIV-RNA in each cohort. Changes in log-transformed plasma HIV-1 RNA from baseline in each cohort after Infusion 1 (a, Day 1), 2 (b, Day 8), and 3 (c, Day 15) of KD-247 are shown with average ± standard deviation (SD) of all cohorts. Each line represents a single patient. Black dotted line shows average ± SD of that observed for the placebo cohort, and red broken line shows the geometric mean changes for each treatment cohort. The average ± SD of the changes in plasma viral load in each cohort are shown with colors: red for 16 mg/kg, blue for 8 mg/kg, green for 4 mg/kg, and purple for placebo. The time points of significant reduction of HIV-1 RNA load are indicated in (d), which corresponds to the time points after Infusion 3, when most of the difference was observed. Changes in plasma HIV-1 RNA from baseline in each cohort throughout the trial are shown in (e). Black dotted line shows the zero level for changes in (e) and (d). Red arrows represent days of infusions. Significance was determined by two-tailed Mann–Whitney U tests. $*P < 0.05$, $**P < 0.01$.

Table 2. Emergence of KD-247 neutralization escape and mismatched variants.

Patient group	Cohort	Patient	Variations of the V3-tip sequence (number of clones)[a]		
			Screening	FU1 (Day 22)	FU5 (Day 99)
Placebo	3	12028	HIGPGRAF (10)	HIGPGRAF (10)	HIGPGRAF (9) HISPGRAF (1)
	3	15008	SIGPGRAF (10)	SIGPGRAF (10)	PIGPGRAF (10)
4mg/kg	1	02009	SIGPGRAF (10)	PIGPGRAF (6) TMGPGRVF (3) PIGPGIMQ (1)	TMGPGRVF (4) PIGPGRAF (3) SIGPGRAF (3)
	1	07007	HIGPGRAF (10)	HIGPGRAF (10)	HIGPGRAF (5) HIGPGRAV(5)
8mg/kg	2	07016	SIGPGRAF (10)	SIGPGRAF (3) TIGPGRAF (3) NIGPGRAF (2) PIGPGRAF (2)	TIGPGRAF (8) SIGPGRAF (1) PIGPGRAF (1)
16mg/kg	3	03017	TIGPGRAF (10)	NMGPGRAF (5) TIGPGKAF (5)	NMGPGRAF (8) TIGPGKAF (2)
	3	12044	HIGPGRAF (10)	HIGPGRAF (9) HIGPGKAF (1)	HIGPGRAF (8) PIGPGRAF (2)

[a]Red letters indicate mismatched variants including escape mutation of R315K.

data suggested that the selection process of the patients appropriate for KD-247 infusion only by V3 genotyping was a limitation. Some primary isolates with reference V3 sequences have a resistance phenotype to KD-247; therefore, involvement of outside V3 for resistance to KD-247 may have accounted for the lack of response [16,17].

Emergence of resistant mutants or mismatched variants

The genotyping test performed for the follow-up samples revealed the emergence of resistant mutants or mismatched variants in seven patients, including two in the placebo cohort (Table 2). Potential switches of coreceptor use were monitored for the 8 and 16 mg/kg cohorts by the Trofile assay. Dual/mixed virus populations of HIV-1 isolates were found in three patients on Day 1. No tropism shifts were observed in the placebo group. Only two patients in the 8 mg/kg cohort had tropism shifts during the study. None of the patients with a tropism shift had significant antiviral response (Supplementary Table 4, http://links.lww.com/QAD/A629).

Discussion

In this phase Ib study, KD-247 was well tolerated and we observed significant decreases in HIV RNA in the 8 and 16 mg/kg KD-247 cohorts. We observed reduction of HIV-1 RNA and viral load set-point in four of six cases in the 16 mg/kg cohort, and long-term suppression of viral load in one patient, despite a significant decrease in plasma concentration of KD-247. It may be necessary to raise the blood concentration of KD-247 to a high level to achieve the initial suppressive effect on viral load. However, maintenance of blood concentration of the antibody may not be essential for a prolonged effect on viral load. In a previous animal model study, KD-247 was administered weekly eight or nine times to monkeys after challenge with pathogenic SHIV. The effects of KD-247 were observed in the lymph node compartment rather than the peripheral blood. The effects of KD-247 on $CD4^+$ T cells in the lymph nodes were observed in a monkey who was unable to maintain the blood concentration of KD-247 because of the emergence of antiidiotype antibody to KD-247 [15]. The observation may partly relate to the prolonged effect of KD-247.

Long-term suppression of viral load observed in one patient (Case #12044) despite a significant decrease in plasma concentration of KD-247 may have interesting implications. Recently, Barouch *et al.* [8] demonstrated the profound therapeutic efficacy of PGT121 and PGT121-containing mAb cocktails in rhesus monkeys chronically infected with SHIV-SF162P3. Virus rebounded in most animals when serum mAb titres declined to undetectable levels, although a subset of animals maintained long-term virological control in the absence of further mAb infusions. Direct antibody-mediated cytotoxic effects on cells chronically infected with HIV-1 were suggested in a humanized mouse model [18]. The phenomenon may be relevant to that observed for Patient #12044 in the present study. The prolonged impact of the neutralizing mAb may partly be owing to the effects other than neutralization, such as antibody-dependent cellular cytotoxicity (ADCC) and antibody-dependent cell-mediated virus inhibition (ADCVI) that can attack virus-producing cells. The importance of nonneutralizing effector activities of bnAbs *in vivo* has been reported in mouse models [19]. Although it is difficult to evaluate ADCC and ADCVI *in vivo*, these

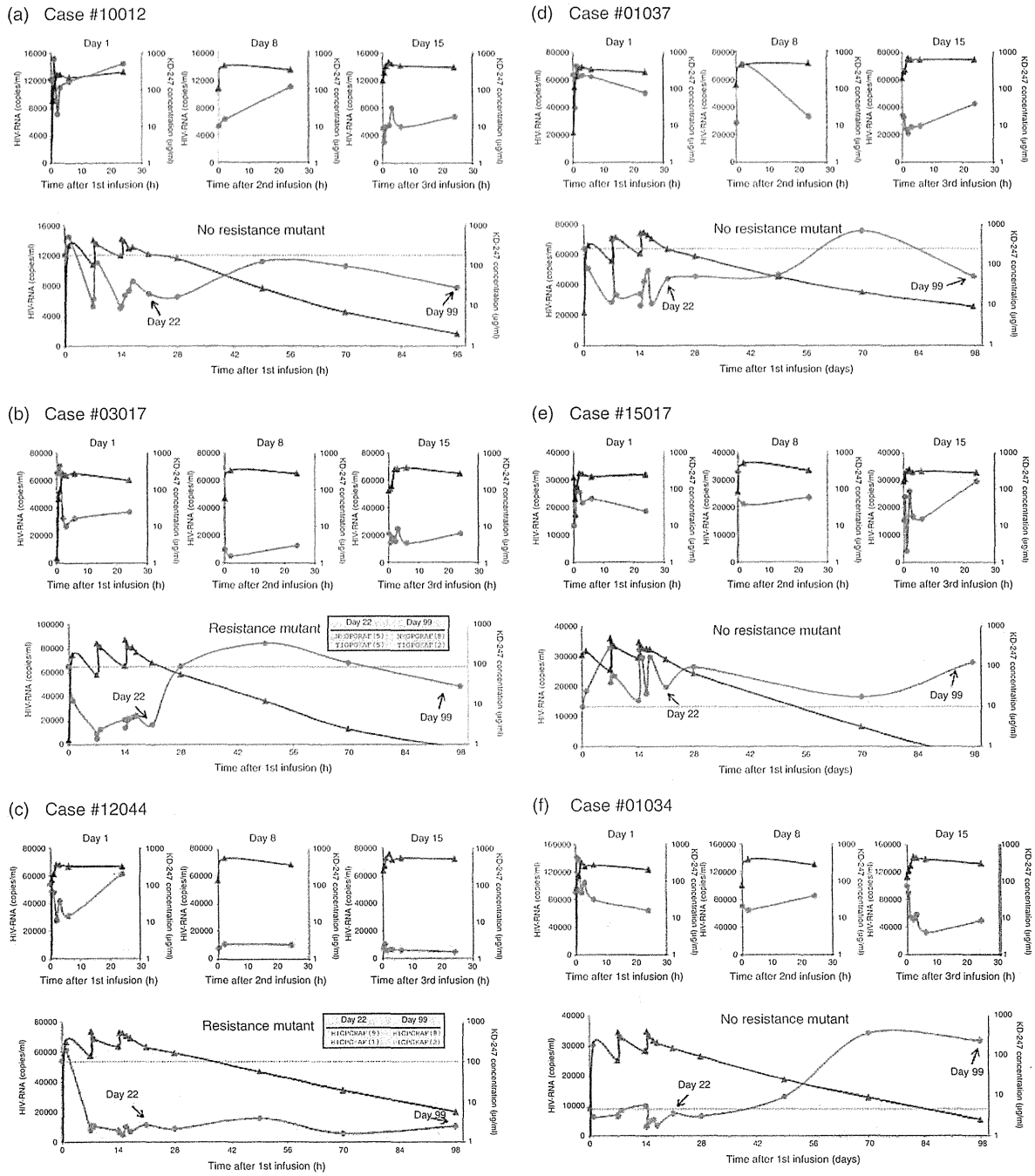

Fig. 3. Longitudinal analysis of HIV-1 RNA reduction and plasma concentration of KD-247 for 16 mg/kg cohort. Plasma concentration of KD-247 is shown as blue triangles with three peaks in an earlier period corresponding to the three infusions of antibody. Plasma HIV RNA is shown as red circles. Emergence of KD-247 resistance mutants with R315K was indicated on Days 22 and 99.

FC-receptor mediated functions were detected for KD-247 *in vitro* (Supplementary Fig. 3, http://links.lww.com/QAD/A629). In addition, secondary immunological responses following viral degradation in antigen-presenting cells by antibody-dependent phagocytosis may have an impact on host antiviral immune responses, including HIV-specific $CD8^+$ T cells, as suggested by the animal model [8]. The enhancement of cell-mediated immunity may in part account for the apparent reduction of viral load set-points after viral rebound from the baseline. We previously reported a KD-247 escape mutant with R315K that showed a less-fit phenotype as compared with the wild-type virus [20]. Although subsequent recovery of the fitness was observed with additional

mutations, fitness cost of the escape mutants may have contributed in part to the reduction of HIV-1 RNA in patients with R315K mutation.

The data in the present clinical trial together with recent studies in animal models [7–9,18] may have an implication for future combination therapy because passive transfer of KD-247 had a significant effect on HIV-1 replication in chronically infected patients. We reported that the neutralization escape mutants to KD-247 became sensitive to chemokine CC receptor (CCR)5 inhibitors [21]. Conversely, resistance mutants to a CCR5 inhibitor, maraviroc, became sensitive to several neutralizing mAbs including KD-247 [22]. Furthermore, a series of in-vitro experiments suggested synergistic effects of the combination of KD-247 and CCR5 antagonists including maraviroc ([21], unpublished observation by S.M. and K.Y.). In view of such a complementary nature of resistance, combination therapy using KD-247 and CCR5 inhibitors warrants future clinical trials. The current results may also imply limitations of monotherapy with conventional antibodies such as KD-247. New-generation bnAbs, especially used in combination, are better candidates for antibody-based treatment in terms of potency and breadth of action. KD-247 may have a role in patients infected with certain viruses that match for neutralization. Combination of KD-247 with certain $CD4^+$-mimetic compounds that markedly enhances the neutralization/binding activity of the antibody may also deserve further investigation [23,24].

Results of this clinical trial should be interpreted with caution because of the small sample size. However, current data and the results from recent primate models taken together warrant further clinical trials of neutralizing mAbs in several different settings with or without ART [25,26].

Acknowledgements

S.M., K.Y. and T.M. designed the study. K.P.R. conducted some of the in-vitro assays for KD-247, including ADCC and ADCVI. J.P. and S.M. led the statistical analysis of the clinical trial. S.M. led the studies and wrote the article with all coauthors. In addition to the authors, the KD-1002 study group includes the following investigators and contributors to the design, conduct or analysis of the study: Principal investigators: E. DeJesus, M. Markowitz, G. Richmond, M. Thompson, R. Liporace, P. Ruane, C. Brinson, K. Staszkow, J. Gathe, Jr., A. Scribner, S. Shoham, H. Marcelin, R. Redfield, T. Sligh and A. Scarsella; and the KD-1002 Protocol Team of Quintiles: E. Vigdorth, J. Bush, C. Gibson G. Breed, D. Despard, P. Ajiboye, B. Tedrow, P. Udeshi, J. Hoglind, R. Rao, R. Kalmadi and A. Armitage.

This work was supported mainly by Kaketsuken and in part by the Ministry of Health, Labour and Welfare of Japan (H22-RPEDMD-G-007 to S.M. and K.Y., H24-AIDS-G-001 and H25-AIDS-G-009 to S.M.) and the Global COE Program, MEXT, Japan.

This study was presented in part at the 7th IAS Conference on HIV Pathogenesis, Treatment and Prevention and IAS Towards an HIV Cure Symposium, Kuala Lumpur Malaysia, 29 June to 3 July 2013, Abstract: OA4-3 LB, TULBPE23.

Conflicts of interest

S.M., K.Y. and K.P.R. declare no competing financial interests. J.P. is an employee of Quintiles Inc. T.M. is an employee of the Chemo-Sero-Therapeutic Research Institute (Kaketsuken). Kaketsuken paid Quintiles to conduct the clinical trial and analyse the results of the study. The authors have no competing interests or other interests that might be perceived to influence the results and/or discussion reported in this article.

References

1. Deeks SG, Autran B, Berkhout B, Benkirane M, Cairns S, Chomont N, *et al.* **Towards an HIV cure: a global scientific strategy.** *Nat Rev Immunol* 2012; **12**:607–614.
2. Forthal DN, Moog C. **Fc receptor-mediated antiviral antibodies.** *Curr Opin HIV AIDS* 2009; **4**:388–393.
3. Overbaugh J, Morris L. **The antibody response against HIV-1.** *Cold Spring Harb Perspect Med* 2012; **2**:a007039.
4. Hessell AJ, Poignard P, Hunter M, Hangartner L, Tehrani DM, Bleeker WK, *et al.* **Effective, low-titer antibody protection against low-dose repeated mucosal SHIV challenge in macaques.** *Nature Med* 2009; **15**:951–954.
5. Mascola JR, Lewis MG, Stiegler G, Harris D, VanCott TC, Hayes D, *et al.* **Protection of Macaques against pathogenic simian/human immunodeficiency virus 89.6PD by passive transfer of neutralizing antibodies.** *J Virol* 1999; **73**:4009–4018.
6. Moldt B, Rakasz EG, Schultz N, Chan-Hui PY, Swiderek K, Weisgrau KL, *et al.* **Highly potent HIV-specific antibody neutralization in vitro translates into effective protection against mucosal SHIV challenge in vivo.** *Proc Natl Acad Sci U S A* 2012; **109**:18921–18925.
7. Klein F, Halper-Stromberg A, Horwitz JA, Gruell H, Scheid JF, Bournazos S, *et al.* **HIV therapy by a combination of broadly neutralizing antibodies in humanized mice.** *Nature* 2012; **492**:118–122.
8. Barouch DH, Whitney JB, Moldt B, Klein F, Oliveira TY, Liu J, *et al.* **Therapeutic efficacy of potent neutralizing HIV-1-specific monoclonal antibodies in SHIV-infected rhesus monkeys.** *Nature* 2013; **503**:224–228.
9. Shingai M, Nishimura Y, Klein F, Mouquet H, Donau OK, Plishka R, *et al.* **Antibody-mediated immunotherapy of macaques chronically infected with SHIV suppresses viraemia.** *Nature* 2013; **503**:277–280.
10. Trkola A, Kuster H, Rusert P, Joos B, Fischer M, Leemann C, *et al.* **Delay of HIV-1 rebound after cessation of antiretroviral therapy through passive transfer of human neutralizing antibodies.** *Nat Med* 2005; **11**:615–622.
11. Mehandru S, Vcelar B, Wrin T, Stiegler G, Joos B, Mohri H, *et al.* **Adjunctive passive immunotherapy in human immunodeficiency virus type 1-infected individuals treated with antiviral therapy during acute and early infection.** *J Virol* 2007; **81**:1016–11031.

12. Eda Y, Takizawa M, Murakami T, Maeda H, Kimachi K, Yonemura H, *et al.* **Sequential immunization with V3 peptides from primary human immunodeficiency virus type 1 produces cross-neutralizing antibodies against primary isolates with a matching narrow-neutralization sequence motif.** *J Virol* 2006; **80**:5552–5562.
13. Eda Y, Murakami T, Ami Y, Nakasone T, Takizawa M, Someya K, *et al.* **Anti-V3 humanized antibody KD-247 effectively suppresses ex vivo generation of human immunodeficiency virus type 1 and affords sterile protection of monkeys against a heterologous simian/human immunodeficiency virus infection.** *J Virol* 2006; **80**:5563–5570.
14. Zolla-Pazner S. **A critical question for HIV vaccine development: which antibodies to induce?** *Science* 2014; **345**:167–168.
15. Murakami T, Eda Y, Nakasone T, Ami Y, Someya K, Yoshino N, *et al.* **Postinfection passive transfer of KD-247 protects against simian/human immunodeficiency virus-induced CD4+ T-cell loss in macaque lymphoid tissue.** *AIDS* 2009; **23**:1485–1494.
16. Shibata J, Yoshimura K, Honda A, Koito A, Murakami T, Matsushita S. **Impact of V2 mutations for escape from a potent neutralizing anti-V3 monoclonal antibody during in vitro selection of a primary HIV-1 isolate.** *J Virol* 2007; **81**:3757–3768.
17. Takizawa M, Miyauchi K, Urano E, Kusagawa S, Kitamura K, Naganawa S, *et al.* **Regulation of the susceptibility of HIV-1 to a neutralizing antibody KD-247 by nonepitope mutations distant from its epitope.** *AIDS* 2011; **25**:2209–2216.
18. Horwitz JA, Halper-Stromberg A, Mouquet H, Gitlin AD, Tretiakova A, Eisenreich TR, *et al.* **HIV-1 suppression and durable control by combining single broadly neutralizing antibodies and antiretroviral drugs in humanized mice.** *Proc Natl Acad Sci U S A* 2013; **110**:16538–16543.
19. Bournazos S, Klein F, Pietzsch J, Seaman MS, Nussenzweig MC, Ravetch JV. **Broadly neutralizing anti-HIV-1 antibodies require Fc effector functions for *in vivo* activity.** *Cell* 2014; **158**:1243–1253.
20. Hatada M, Yoshimura K, Harada S, Kawanami Y, Shibata J, Matsushita S. **Human immunodeficiency virus type 1 evasion of a neutralizing anti-V3 antibody involves acquisition of a potential glycosylation site in V2.** *J Gen Virol* 2010; **91**:1335–1345.
21. Yoshimura K, Shibata J, Kimura T, Honda A, Maeda Y, Koito A, *et al.* **Resistance profile of a neutralizing anti-HIV monoclonal antibody, KD-247, that shows favourable synergism with anti-CCR5 inhibitors.** *AIDS* 2006; **20**:2065–2073.
22. Yoshimura K, Harada S, Boonchawalit S, Kawanami Y, Matsushita S. **Impact of maraviroc-resistant and low-CCR5-adapted mutations induced by in vitro passage on sensitivity to antienvelope neutralizing antibodies.** *J Gen Virol* 2014; **95**:1816–1826.
23. Yoshimura K, Harada S, Shibata J, Hatada M, Yamada Y, Ochiai C, *et al.* **Enhanced exposure of human immunodeficiency virus type 1 primary isolate neutralization epitopes through binding of CD4 mimetic compounds.** *J Virol* 2010; **84**:7558–7568.
24. Madani N, Princiotto AM, Schon A, LaLonde J, Feng Y, Freire E, *et al.* **CD4-mimetic small molecules sensitize human immunodeficiency virus to vaccine-elicited antibodies.** *J Virol* 2014; **88**:6542–6555.
25. Klein F, Mouquet H, Dosenovic P, Scheid JF, Scharf L, Nussenzweig MC. **Antibodies in HIV-1 vaccine development and therapy.** *Science* 2013; **341**:1199–1204.
26. Picker LJ, Deeks SG. **Antibodies advance the search for a cure.** *Nature* 2013; **503**:207–208.

Virology 475 (2015) 187–203

Contents lists available at ScienceDirect

Virology

journal homepage: www.elsevier.com/locate/yviro

Complementary and synergistic activities of anti-V3, CD4bs and CD4i antibodies derived from a single individual can cover a wide range of HIV-1 strains

Kristel Paola Ramirez Valdez [a], Takeo Kuwata [a], Yasuhiro Maruta [a], Kazuki Tanaka [a], Muntasir Alam [a], Kazuhisa Yoshimura [a,b], Shuzo Matsushita [a,*]

[a] Matsushita Project Laboratory, Center for AIDS Research, Kumamoto University, Kumamoto, Japan
[b] AIDS Research Center, National Institute of Infectious Diseases, Tokyo, Japan

ARTICLE INFO

Article history:
Received 24 September 2014
Returned to author for revisions
17 October 2014
Accepted 10 November 2014
Available online 5 December 2014

Keywords:
HIV-1
Conventional antibodies
Neutralizing antibodies
Synergy
ADCC activity

ABSTRACT

Antibodies with modest neutralizing activity and narrow breadth are commonly elicited in HIV-1. Here, we evaluated the complementary and synergistic activities of a set of monoclonal antibodies (MAb) isolated from a single patient, directed to V3, CD4 binding site (CD4bs), and CD4 induced (CD4i) epitopes. Despite low somatic hypermutation percentages in the variable regions, these MAbs covered viral strains from subtypes B, C, A and CRF01_AE and transmitted/founder viruses in terms of binding, neutralizing and antibody-dependent cell-mediated cytotoxicity (ADCC) activities. In addition, a combination of the anti-V3 and CD4bs MAbs showed a synergistic effect over the neutralization of HIV-1_{JR-FL}. A humoral response from a single patient covered a wide range of viruses by complementary and synergistic activities of antibodies with different specificities. Inducing a set of narrow neutralizing antibodies, easier to induce than the broadly neutralizing antibodies, could be a strategy for developing an effective vaccine against HIV-1.

Introduction

Despite the great advances in the treatment of HIV-1 infection, there are still major obstacles to effective control of HIV-1 infection. Active replication persistence and immune activation under suppressive highly active antiretroviral therapy (HAART) (Buzon et al., 2010; Palmer et al., 2008; Richman et al., 2009), secondary effects of the drugs (Montessori et al., 2004; Reust, 2011), and the socio-economic burden of long-term treatment (Boyer, 2009; Naik et al., 2009) are still present; making the development of a protective vaccine desirable. Neutralizing antibodies are an important component of a protective vaccine-induced immune responses and much effort has been focused on the development of broadly neutralizing antibodies against conserved epitopes on the functional Env trimer of HIV-1 (Bonsignori et al., 2011; Corti et al., 2010; Walker et al., 2009).

Advances in antibody technology have uncovered broadly neutralizing Abs (bNAbs) (Marasco and Sui, 2007; Zhu et al., 2013; Zuo et al., 2011) and their efficacy has been proved in non-human animal models. Protection from infection by Simian immunodeficiency virus (SIV) was correlated with the humoral response produced after vaccination with Env and/or Gag and Pol of rhesus macaques (Barouch et al., 2013; Roederer et al., 2014). Protection was also observed in rhesus macaques vaccinated with Env derived peptides and challenged with chimeric simian-human immunodeficiency viruses (SHIV) $SHIV_{162P3}$ and $SHIV_{C2/1}$ (DeVico et al., 2007; Eda et al., 2006a). Passive administration of antibodies was also proved useful in protecting for and controlling SHIV and HIV-1 infection. In rhesus macaques chronically infected with $SHIV_{162P3}$, passive administration of bNAbs (PGT121, 3BNC117 and b12 combined or alone) reduced viral load and resulted in control of the infection (Barouch et al., 2013; Ng et al., 2010). Similar results were observed in humanized mice chronically infected with HIV-1_{YU2} after the passive administration of bNAbs 45–46^{G54W}, PG16, PGT128, 10-1074 and 3BC176 (Klein et al., 2012). Passive administration of MAbs PGT121, b12, 2G12, 2F5 and 4E10 also offered protection from infection with SHIV (Hessell et al., 2010, 2009a, 2009b; Mascola et al., 2000, 1999; Moldt et al., 2012; Parren et al., 2001) even when the antibody (b12) was administered topically (Veazey et al., 2003); or when the administered antibodies were purified IgG from infected chimpanzees (Shibata et al., 1999).

It has been proposed that an immunization strategy that could elicit such antibodies would be protective in humans (Stamatatos

* Corresponding author. Fax: +81 96 373 6537.
E-mail address: shuzo@kumamoto-u.ac.jp (S. Matsushita).

http://dx.doi.org/10.1016/j.virol.2014.11.011
0042-6822/

et al., 2009); however, to date there is no vaccine that induces their production.

In naturally infected HIV-1 patients, bNAbs are not commonly produced; instead, antibodies are often directed against strain-specific or non-neutralizing sites in Env (Burton et al., 1991; Corti et al., 2010). Only 10 to 25% of HIV-1-infected individuals generate neutralizing antibodies, and a minority of these individuals, approximately around 1%, is considered elite neutralizers, besides, bNAbs appear late (1 to 3 years) after infection (Binley et al., 2008; Deeks et al., 2006; Dhillon et al., 2007; Doria-Rose et al., 2010, 2009; Gray et al., 2011; Sather et al., 2009; Simek et al., 2009) and frequently harbor uncommon characteristics which probably pose obstacles to their generation, including high levels of somatic mutations, long heavy-chain complementarity-determining regions 3 (CDRH3s), frequent insertions or deletions, and high levels of polyreactivity (Haynes et al., 2012b; Huber et al., 2010; Klein et al., 2013; Scheid et al., 2011; Sok et al., 2013; Xiao et al., 2009). Moreover, when the immunoglobulin sequences of bNAbs are experimentally reverted to their germline precursors, as they are found on naive B cells, binding to HIV-1 Env is often significantly diminished or even completely abrogated (Bonsignori et al., 2011; Haynes et al., 2012b; McGuire et al., 2014; Scheid et al., 2011; Wu et al., 2011; Xiao et al., 2009). This suggests difficulties in inducing bNAbs in HIV-1-infected patients and also by vaccination, because many rounds of affinity maturation are required which means that immunizations should be repeated many times as well.

Antibodies to the V3 loop, CD4bs and CD4i have been produced by HIV infection or vaccination, but neutralization by these antibodies is generally not broadly effective for preventing HIV-1 infection because of steric constraints blocking the access of these antibodies to the epitopes, and mutations in their epitopes that allow to escape from these antibodies. However, these modest neutralizing antibodies appear faster after infection (even as early as 2 weeks after sero-conversion) and are also capable of exert pressure over the virus (Bar et al., 2012; Haynes et al., 2012b; McGuire et al., 2014; Overbaugh and Morris, 2012; Pollara et al., 2014).

Besides neutralization, non-neutralizing responses, specifically the ADCC activity has been associated with protection from HIV. The most remarkable case is the RV144 trial result, which showed a 31.2% of vaccine efficacy (Rerks-Ngarm et al., 2009) and it has been proposed that the ADCC activity of V1/V2 antibodies induced by the vaccine may be the most important correlation for protection (Haynes et al., 2012a; Rerks-Ngarm et al., 2009; Wren et al., 2012). Vaccination in animal models has shown similar results (Hessell et al., 2007; Xiao et al., 2010) and it has also been reported that broader ADCC responses correlate with long-term control of HIV, slow progression of disease and lower viremia (Nag et al., 2004; Wren et al., 2013; Xiao et al., 2010).

It is certainly desirable for HIV-vaccines to induce antibodies that neutralize global isolates of diverse subtypes. However, in view of the difficulty in inducing bNabs in uninfected subjects, the induction of a complementary set of antibodies with limited neutralizing activity may be an attainable alternative approach. We have been following a single patient infected with HIV that has a cross-neutralizing activity to a variety of HIV-1 isolates including a panel of clinical isolates belonging to subtypes B, C, CRF01_AE and A. The patient is a hemophiliac who has been infected with HIV-1 for more than 25 years without any antiretroviral treatment. To elucidate the mechanism to control viruses in this patient we established a series of MAbs and demonstrated that a combination of antibodies to the V3 loop, CD4bs and CD4i covered effectively a wide range of viruses by their complementary and synergistic activities.

Results

Isolation and classification of monoclonal antibodies from an HIV-1 infected patient with long-term non-progressive disease

A total of 1718 B-cell clones were established by Epstein-Barr virus (EBV) transformation from the patient KTS376 who has had controlled HIV-1 infection for more than 25 years without any

Table 1
Subclass, target and genetic characteristics of human monoclonal antibodies against HIV-1 obtained from a patient with non-progressive disease.

No	Clone	Subclass	Target	Gene usage		Somatic mutation (%)		CDRH3 length
				VH	VL	VH	VL	
1	0.5γ (1C10)	IgG1κ	V3	VH3-30	VK2-28	10.8	4.1	18
2	1D9	IgG1κ	V3	VH3-30	VK2-28	12.8	3.5	16
3	5G2	IgG1κ	V3	VH3-30	VK2-28	12.8	6.5	16
4	16G6	IgG1λ	V3	VH5-51	VL3-19	4.9	6.4	7
5	717G2	IgG2κ	V3	VH3-30	VK2D-29	10.8	7.1	21
6	2F8	IgG1λ	V3	–	–	–	–	–
7	3E4	IgG1κ	V3	–	–	–	–	–
8	3G8	IgG1κ	V3	–	–	–	–	–
9	42F9	IgG1κ	CD4bs	VH3-20	VK1-39	2	2.5	19
10	49G2	IgG1λ	CD4bs	VH1-18	VL1-44	5.9	1.8	22
11	82D5	IgG1λ	CD4bs	VH1-18	VL1-44	6.2	1.7	22
12	0.5δ(3D6)	IgG1λ	CD4bs	–	–	–	–	–
13	4E3	IgG1κ	CD4bs	–	–	–	–	–
14	7B5	IgG2λ	CD4bs	–	–	–	–	–
15	4E9C	IgG1κ	CD4i	VH1-69	VK3-15	6.6	1.8	22
16	916B2	IgG1λ	CD4i	VH1-69	VL7-46	8.7	5.9	16
17	917B11	IgG1λ	CD4i	VH1-69	VL1-51	5.9	2.8	28
18	4C11	IgG1λ	CD4i	–	–	–	–	–
19	5D6S	IgG1κ	CD4i	VH1-69	VK3-20	9.3	9.6	26
20	7F11	IgG2κ	CD4i	–	–	–	–	–
21	5E8	IgG2κ	–	–	–	–	–	–
22	7B9N	IgG3κ	–	–	–	–	–	–
23	9F7	IgG1κ	–	–	–	–	–	–
24	39D5	IgG3κ	–	–	–	–	–	–
25	43D7	IgG2κ	–	–	–	–	–	–

VH: Variable heavy chain. VL: Variable light chain. CDRH3: Third complementary determinant region of the heavy chain. Not determine.

antiretroviral treatment. Out of these B cell clones, we identified 25 clones continuously producing MAbs reactive to gp120 (Table 1). First, MAbs were examined for their reactivity to the V3-peptide corresponding to the V3-region of the $gp120_{JR-FL}$ (NNT20) and the reactive MAbs, 0.5γ, 1D9, 2F8, 3E4, 3G8, 5G2, 717G2 and 16G6, were classified as anti-V3 antibodies. Later, using a set of peptides that have different V3 sequences and overlapping short peptides, we identified the minimum epitope and the cross-reactivity of these antibodies (Supplementary Table 1). The reactivity of these MAbs to short peptides was decreased, and only 1D9 and 5G2 bound to 10 mer peptides. Although 2F8 did not recognize any overlapping short peptides, this MAb was capable to bind to the V3 peptide from NSI, correspondent to the CRF01_AE subtype.

MAbs other than anti-V3 were classified in three groups according to the effect of soluble CD4 (sCD4) on the reactivity to gp120: CD4bs, CD4i and other epitopes (Figs. 1 and 2). MAbs, 0.5δ, 4E3, 7B5, 42F9, 49G2 and 82D5, were classified as CD4bs antibodies according to the reduction of reactivity in the presence of sCD4. MAbs, 4C11, 4E9C, 5D6S, 7F11, 916B2 and 917B11, were classified as CD4i antibodies according to the enhancement effect by sCD4. The rest of MAbs, which did not react to the V3 peptide and did not show enhancement or inhibition by sCD4, were classified as MAbs to other epitopes. Anti-V3 MAb, KD-247 (Eda et al., 2006a), CD4bs MAb, b12 (Burton et al., 1991) and CD4i MAbs, 17b (Thali et al., 1993) were also analyzed as controls.

For the anti-V3 antibodies, no influence in their binding to monomeric gp120 was noted in the presence of sCD4 when analyzed by ELISA (Fig. 1). However, the enhanced reactivity by sCD4 was observed against Env on the cell surface in most of anti-V3 MAbs (Fig. 2). This is consistent with the previous reports (Huang et al., 2005; Thali et al., 1993), which showed that the binding of CD4 to gp120 caused the V3 to protrude and became more available, particularly in the strains that use the CCR5 co-receptor. Although a reduction of reactivity was observed for the CD4bs MAbs in ELISA, this reduction of reactivity against trimeric Env was not obvious in the MAbs, such as 4E3 and 49G2 (Fig. 2). The enhanced reactivity by sCD4 was observed in all the CD4i MAbs, both in ELISA and flow cytometry analysis (Figs. 1 and 2) as previously reported for the CD4i MAbs (Lusso et al., 2005; Mbah et al., 2001; Wu et al., 2008). The MAbs to other epitopes did not show reactivity to trimeric Env, suggesting that these MAbs recognized the unexposed region of the Env trimer (Fig. 2).

Genetic characterization of MAbs

Generally, gp120 epitope reactivity is mediated by IgG1, although IgG2 can also be found (Banerjee et al., 2010). MAbs predominantly consisted of IgG1. IgG3 was observed only in the "other epitope" group, and none of the antibodies isolated was IgG4 (Table 1). Representative MAbs were genetically cloned, and gene usage, somatic mutation percentage and CDRH3 length was determined (Table 1). Anti-V3 antibodies showed a marked preference of the usage of the VH3-30 gene for the variable region of the heavy chain (VH) and VK2-28 for the variable region of the light chain (VL); and only the MAb 16G6 used the VH5-51 gene and λ light chain, which were previously reported as preferential gene usage by anti-V3 antibodies (Gorny et al., 2009). All the anti-V3 antibodies analyzed had the V to I substitution in position 55 (IMGT unique numbering) of FR2 (Supplementary Fig. 1). MAbs, 1D9 and 5G2, used the same genes and the length of CDRH3 was also the same among them. These characteristics, as well as the close similarity in their sequences (Supplementary Fig. 1), suggested that these two MAbs originated from a common ancestor. In contrast, 0.5γ, which used the same genes as 1D9 and 5G2, was considered as from another lineage, because 0.5γ had the CDRH3 different from 1D9 and 5G2 in terms of length and sequences (Table 1 and Supplementary Fig. 1). Two of the three CD4bs MAbs used the same genes, VH1-18 and VL1-44, suggesting that these MAbs had the same origin. All four of the CD4i MAbs analyzed used the VH1-69 gene, which is consistent with previous reports (Gorny et al., 2009; Huang et al., 2004), but did not use the same light chain gene. This indicates that CD4i antibodies with the VH1-69 gene were

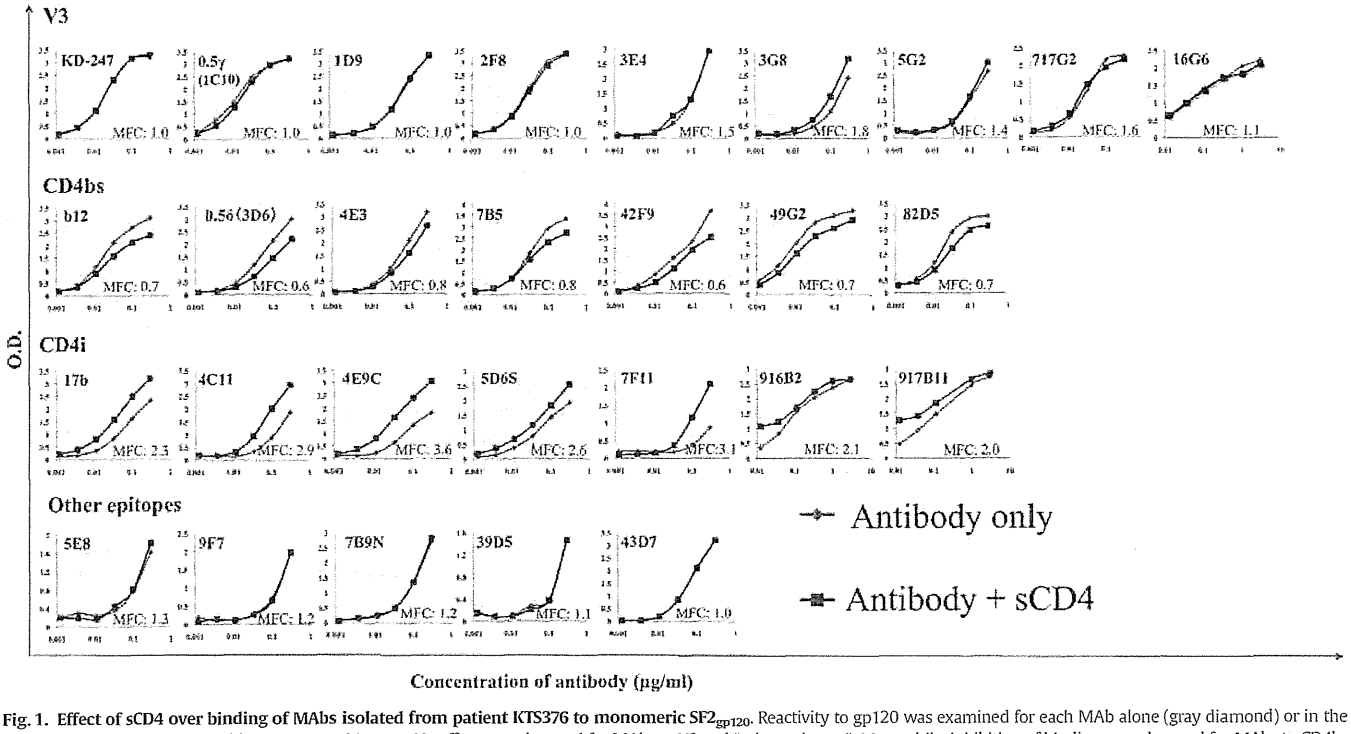

Fig. 1. Effect of sCD4 over binding of MAbs isolated from patient KTS376 to monomeric $SF2_{gp120}$. Reactivity to gp120 was examined for each MAb alone (gray diamond) or in the presence of sCD4 (black square) by capture ELISA assay. No effect was observed for MAbs to V3 and "other epitopes". Meanwhile, inhibition of binding was observed for MAbs to CD4bs and enhancement of binding was observed for MAbs to CD4i epitope. Maximum fold change (MFC) was calculated as follows: O.D. sCD4 positive/ O.D. sCD4 negative.

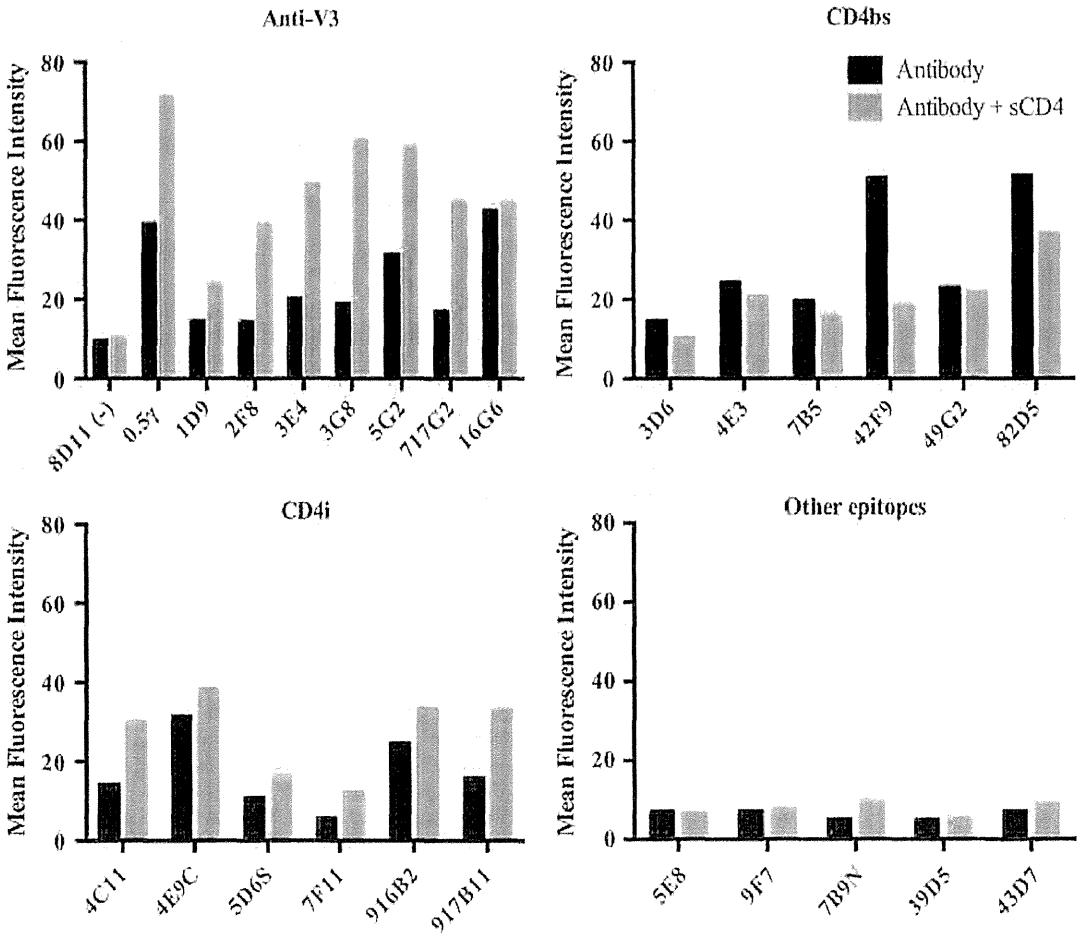

Fig. 2. Binding of MAbs from patient KTS376 to Env expressed on the surface of cells. Reactivity to PM1/CCR5 cells chronically infected with HIV-$1_{JR\text{-}FL}$ was analyzed using flow cytometer. Mean fluorescence intensity is shown for each MAb in the presence (gray) or absence (black) of sCD4. Enhancement of binding was observed for most of the MAbs to V3 and all the CD4i MAbs when sCD4 was added. Inhibition of binding was observed for MAbs to CD4bs in the presence of sCD4. MAbs to other epitopes did not bind to trimeric Env on the cell surface.

frequently induced during infection. Abundance of tyrosines (Y) in CDHR3, which was reported previously in CD4i antibodies (Choe et al., 2003; Huang et al., 2004; Xiang et al., 2002) was present not only in CD4i MAbs but also in CD4bs MAbs. These results suggest that antibodies with preferential genes were abundantly induced in the patient KTS376, and that dominant antibody lineages were observed in the V3 and CD4bs antibodies.

Mostly, somatic hypermutation percentages were higher in VH than in VL, with the exceptions of 16G6 and 42F9 (Table 1). Overall somatic hypermutation percentages were relatively low (VH mean: 7.9% and VL mean: 4.0%) contrasting with the levels of somatic hypermutations reported for bNAbs. For example, mutation percentages of bNAbs HJ16, 2G12 and b12 were between 20 and 45% for VH and between 17 and 30% for VL; while the relatively less hypermutated bNAbs PG6 and PG9 showed percentages of 21.4% and 18.8% for VH and 21.2 and 14.1% for the VL, respectively (Klein et al., 2013; Sok et al., 2013; Wu et al., 2011; Zhou et al., 2010). The low somatic mutation percentages observed for the MAbs isolated from KTS376 corresponded to those reported for the "conventional antibodies" against HIV-1 (Zolla-Pazner, 2014).

Binding activities of the MAbs to various HIV-1 Envs

Cross-reactivity of MAbs was examined using Envs from various HIV-1 strains (Fig. 3). All the MAbs tested bound to Env from most of subtype B viruses including laboratory strains (89.6, SF162 and YU2) and primary viruses including T/F viruses (WITO and RHPA), 6535.3 (SVPB5) and REJO4541.67 (SVPB16) (Fig. 3). The Env of the laboratory strain, NL4-3, was reactive to all the CD4bs and CD4i MAbs, but not to any of the V3 MAbs, consistent with the results observed in the V3-peptide ELISA (Supplementary Table 1 and Fig. 3). Cross-subtype binding activities against subtype A, CRF01_AE and subtype C were observed in most of CD4bs and CD4i MAbs, while most V3 MAbs exhibited significantly lower cross-subtype binding activities than CD4bs and CD4i MAbs (Fig. 3, Supplementary Fig. 2). Of the V3 antibodies, 16G6 bound all the subtype C viruses tested, and showed a considerable cross-reactivity compared with other V3 MAbs. This is consistent with the previous reports that antibodies encoded by the VH5-51/VLλ genes can recognize Envs from various subtypes (Gorny et al., 2011). These results demonstrated that these MAbs isolated from a single patient, as a set of MAbs, covered a wide range of viruses including B and other subtypes. The lack of reactivity of some MAbs was complemented with the activity of other MAbs, and at least two of the three epitopes tested (V3, CD4bs and CD4i) were recognized by these MAbs.

Neutralizing activities of the MAbs against various HIV-1 subtypes

To evaluate the neutralizing activity of these MAbs, we first used representative HIV-1 subtype B laboratory and primary isolates (Fig. 4). The neutralizing activity against SF162 and BaL

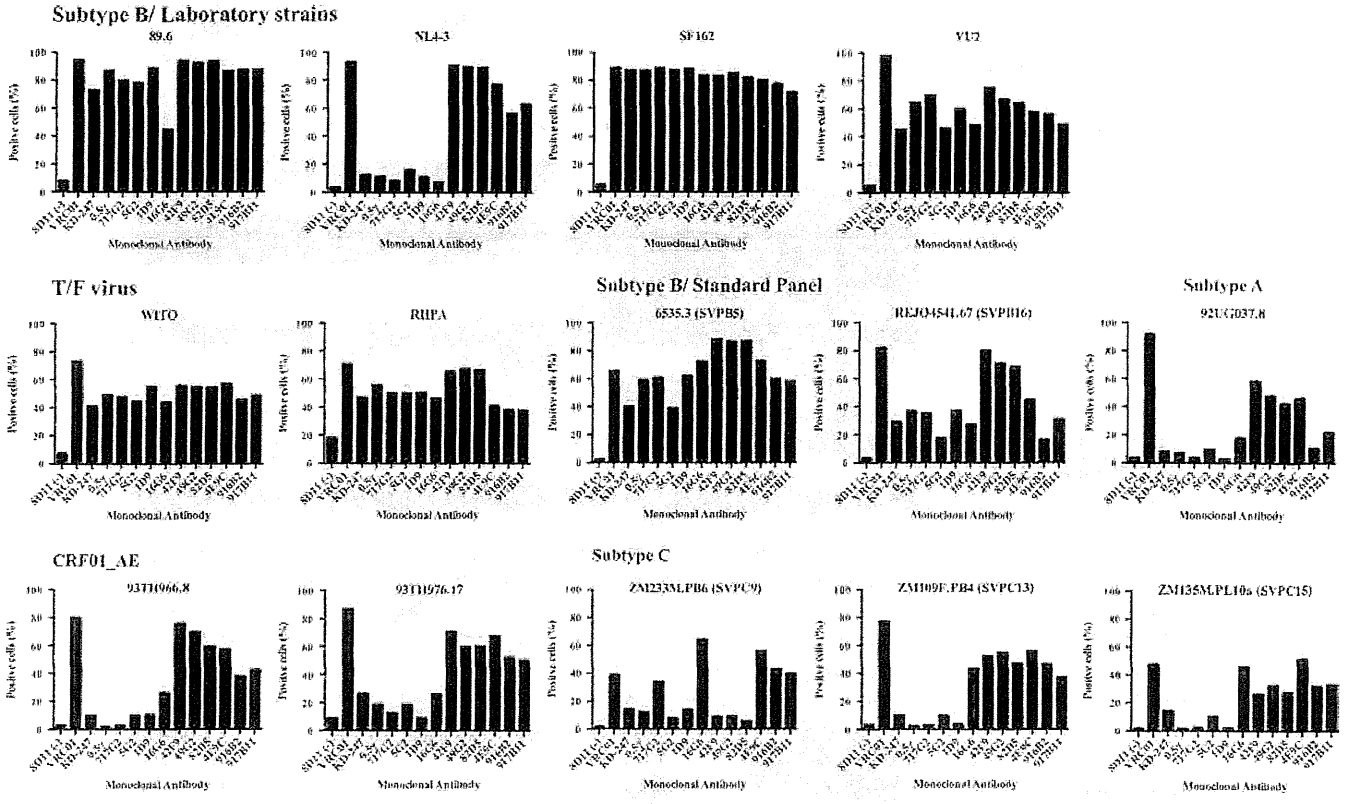

Fig. 3. Cross-reactivity of MAbs from patient KTS376 to Env from various HIV-1 strains. Reactivity to Env from various HIV-1 strains, such as laboratory strains, transmitted/founder (T/F) viruses and viruses belonging to subtype A, B, C and CRF01_AE, was analyzed by flow cytometry using transfected 293T cells. Percentages of cells recognized by MAbs are shown. Controls of the assay included the monoclonal IgG 8D11 (negative control), VRC01 and KD-247 (positive controls). MAbs to V3 potently bound to cells expressing Envs from all the subtype B viruses tested, with the exception of NL4-3. MAbs to CD4bs and CD4i showed a greater cross-subtype reactivity more than MAbs to V3 MAbs.

was observed for all MAbs tested, consistent with the results of binding activity. Most of the V3 MAbs, with the exception of 16G6, showed a potent neutralization of laboratory strains other than IIIB, and 0.5γ, 717G2 and 1D9 were also effective against primary isolates. Although 16G6 reacted to many viruses (Fig. 3), the neutralizing activity of this MAb was weak and narrow. The CD4bs and CD4i MAbs neutralized HIV-1 IIIB, which was resistant to the neutralization by most of the V3 antibodies because of the two amino acid insertion adjacent to the V3-tip, while the potency and spectrum of the CD4bs and CD4i MAbs were low and narrow, compared with those of V3 MAbs. Especially, KTS376-96, the autologous virus from the patient that MAbs were isolated, was sensitive to V3 MAbs, but not to the CD4i or CD4bs MAbs at all. These results suggest that the V3 antibodies mainly neutralized the viruses present in this patient.

To further evaluate the neutralizing activity of the MAbs, we used a panel of pseudo-typed viruses named standard panel viruses subtype B (SVPB) and C (SVPC) (Li et al., 2006, 2005) (Fig. 4), and one subtype A and two CRF01_AE pseudoviruses. As shown in Fig. 4, 0.5γ was highly effective against subtype B viruses, and 10 out of 12 SVPB viruses were neutralized by 0.5γ with a half maximal inhibitory concentration (IC_{50}) below 150 μg/ml. The coverage of subtype B viruses by 1D9 was lower than for 0.5γ, but 1D9 showed a cross-subtype neutralization against ZM53M.PB12 (subtype C) and 92UG037.8 (subtype A). Consistent with the results of neutralization of laboratory and primary strains, the potency of CD4bs and CD4i MAbs were low and narrow against standard panel viruses. However, THRO4156.18 (subtype B), which was reported as a neutralizing resistant virus (Li et al., 2005), was neutralized by the CD4bs MAbs 49G2 and 42F9. In addition, TRO.11 (subtype B) and CAAN5342.A2 (subtype B), which were not neutralized by the V3 MAbs other than 0.5γ, were sensitive to CD4bs MAb 49G2 and CD4i MAb, 4E9C, respectively. Moreover, cross-subtype neutralization activity was higher in the CD4bs and CD4i MAbs, which neutralized 4 subtype C viruses, than the V3 MAbs. CD4bs MAb 49G2 and CD4i MAb 4E9C significantly contributed to the cross-subtype neutralization, and five out of 12 SVPC viruses (42%) were neutralized by this set of MAbs.

We also evaluated the neutralizing activity of these MAbs against 10T/F viruses of subtype B (Fig. 4) (Keele et al., 2008; Lee et al., 2009; Ochsenbauer et al., 2012; Salazar-Gonzalez et al., 2009, 2008). Anti-V3 MAbs neutralized 6 out of the 10 analyzed T/F viruses, and CD4i MAb 49G2 neutralized SUMA, which in contrast to V3 MAbs did not neutralize. Interestingly, 5G2, which showed relatively weak and narrow neutralizing activity against other viruses, showed considerable neutralization against T/F viruses. As a result, MAbs from a single patient provided coverage of 70% of the analyzed T/F viruses.

Plasma from KTS376 obtained in two different time points (2002 and 2005) was able to recapitulate the neutralizing activity of the monoclonal antibodies when confronted with representative viruses from subtype B, C and CRF01_AE (Supplementary Fig. 2).

These results demonstrated that MAbs from patient KTS376 neutralized a broad range of viruses. Although the coverage of each MAb was limited, in combination they covered a considerable number of viruses from different subtypes and origins. Anti-V3 antibodies mainly provided potency and broadness against viruses inside subtype B, while CD4bs and CD4i MAbs complementarily covered viruses that V3 antibodies did not neutralize, especially non-subtype B viruses.